



NGC 2237-9 The Rosette Nebula

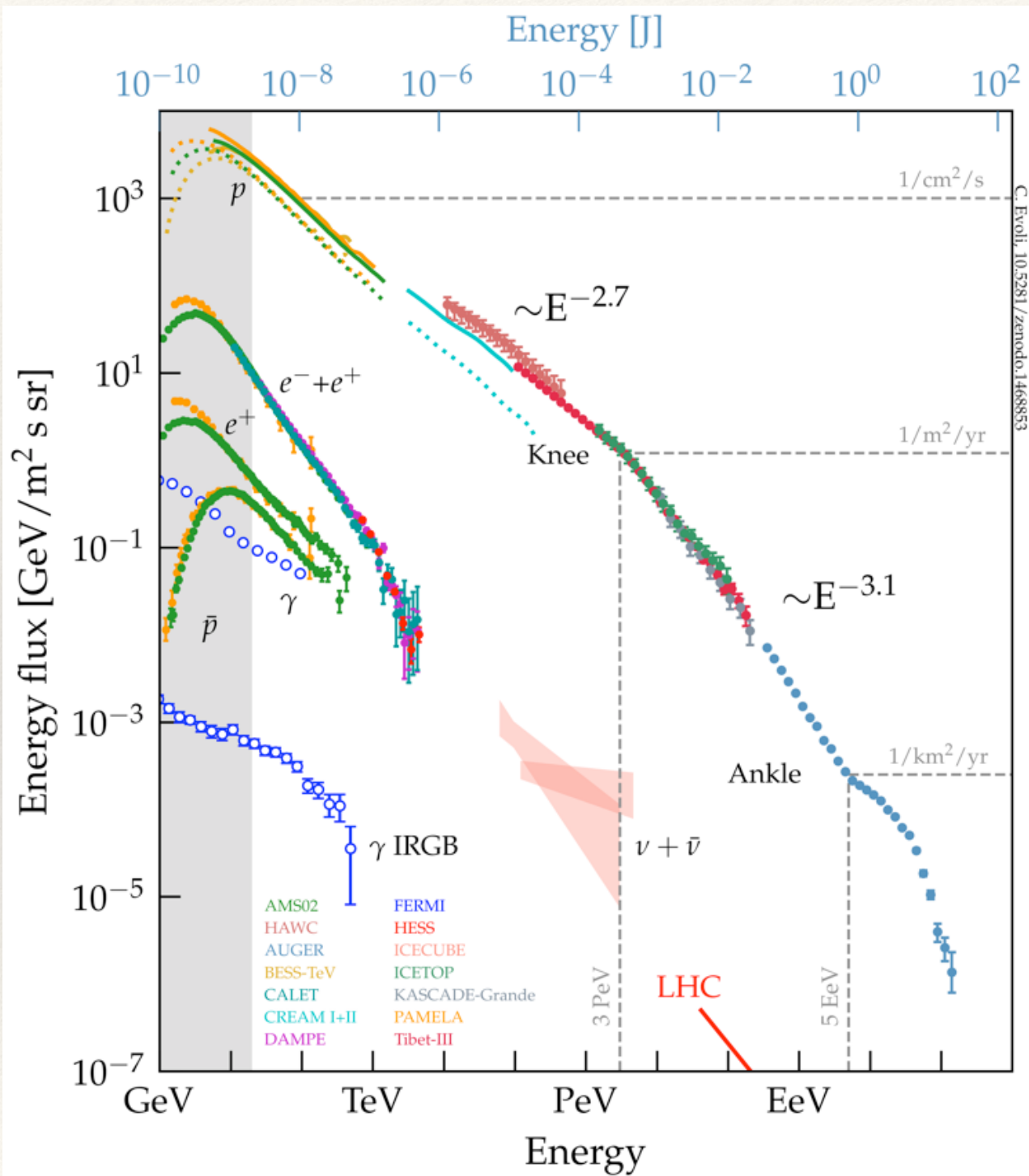
HONEST online Meeting - November 30th 2022

Stellar Clusters as PeVatrons: Cosmic Ray acceleration

Giovanni Morlino
INAF / Oss. Astrofisico di Arcetri
Firenze
ITALY



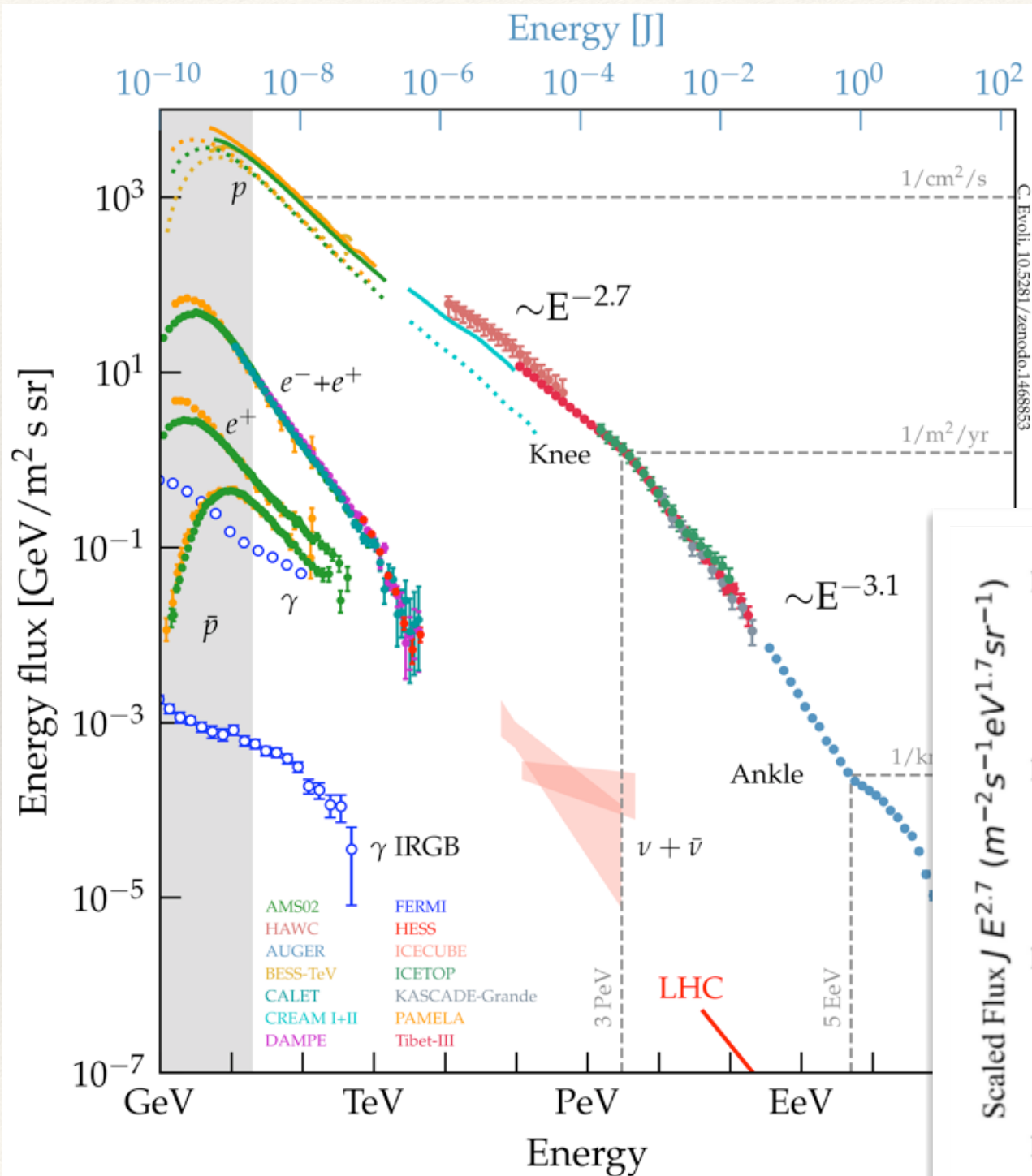
How to explain the origin of Galactic CRs



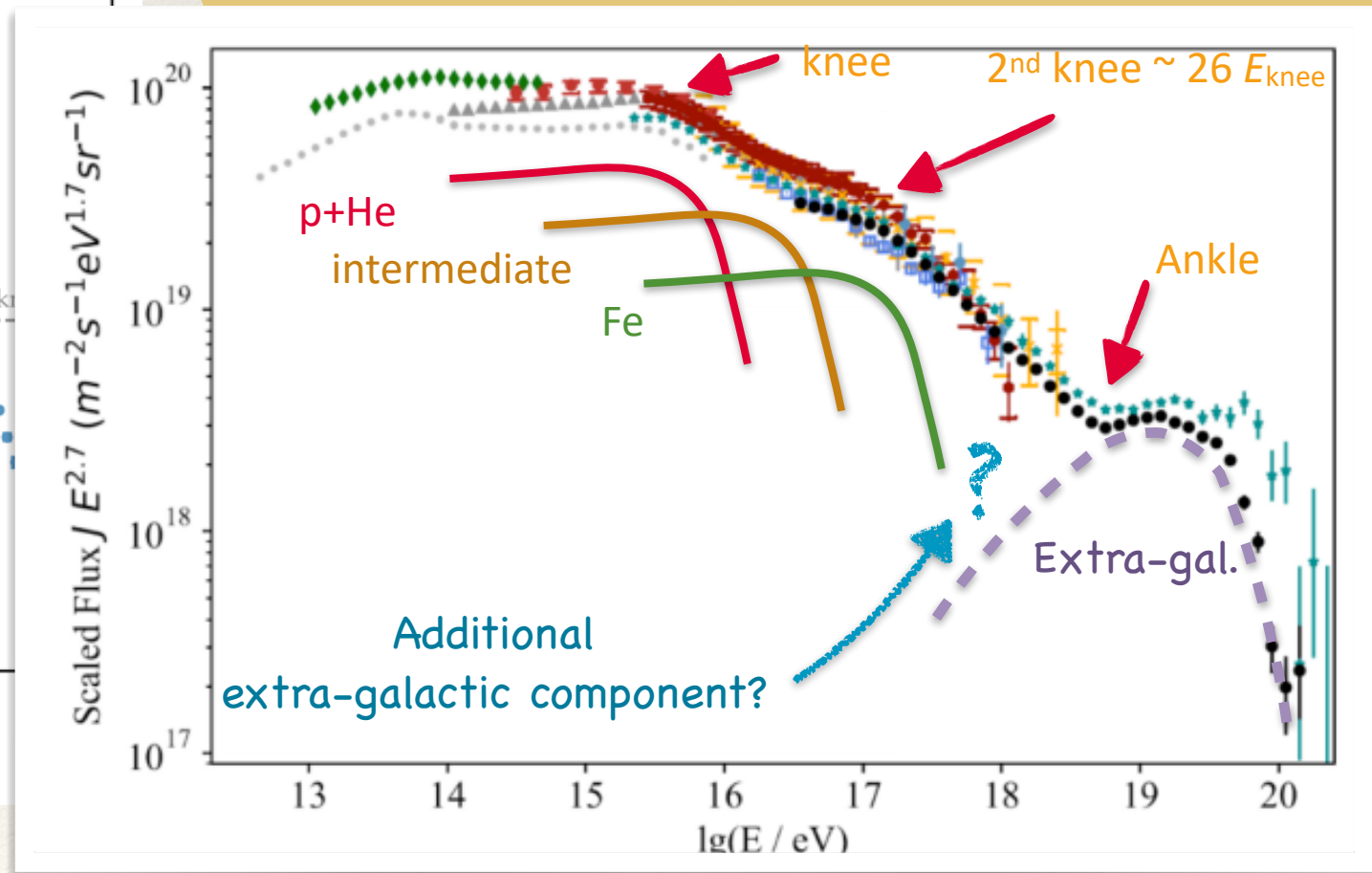
Requirements for sources

- ❖ Energetics: $\sim 10^{40}$ erg/s
- ❖ Injected spectrum < PeV: $\propto E^{-2.3}$
- ❖ Maximum energy (p): $\gtrsim 10^{15}$ eV
- ❖ Anisotropy: $\sim 10^{-3}$ @ 10 TeV
- ❖ Composition: few anomalies w.r.t. Solar

How to explain the origin of Galactic CRs



- ### Requirements for sources
- ❖ Energetics: $\sim 10^{40}$ erg/s
 - ❖ Injected spectrum < PeV: $\propto E^{-2.3}$
 - ❖ Maximum energy (p): $\gtrsim 10^{15}$ eV
 - ❖ Anisotropy: $\sim 10^{-3}$ @ 10 TeV
 - ❖ Composition: few anomalies w.r.t. Solar



The most popular scenario: DSA@SNR shocks

❖ Why supernova remnant are so popular?

1. Enough power to sustain the CR flux ($\sim 10\%$ of kinetic energy)
2. Spatial distribution of SNRs compatible with CR distribution (inferred from diffuse gamma-ray emission)
3. Enough sources to explain anisotropy
4. Observations show the presence of non thermal particles
5. A well developed theory for particle acceleration (DSA)

❖ However

- **No evidence of acceleration beyond ~ 100 TeV even in very young SNRs**
- **From theory only very powerful and rare SNRs can reach PeV** (see talk by Bell and Reville)
- Anomalous CR composition cannot be easily explained (see talk by Gabici)
- Spectral anomalies (p, He, CNO have different slopes)
- etc...

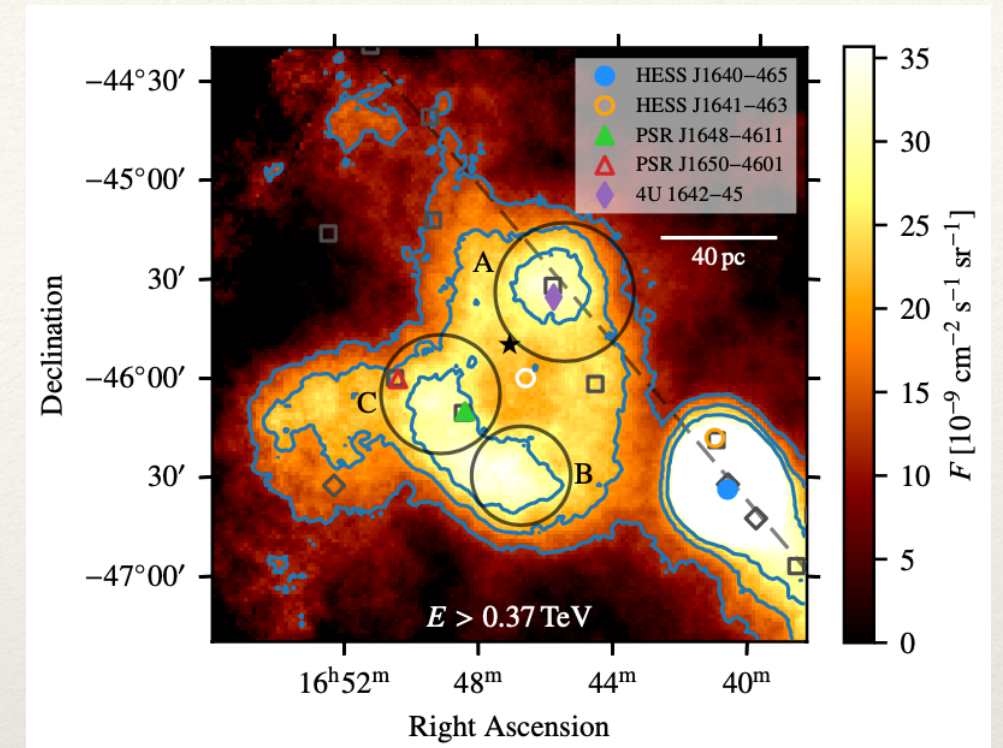
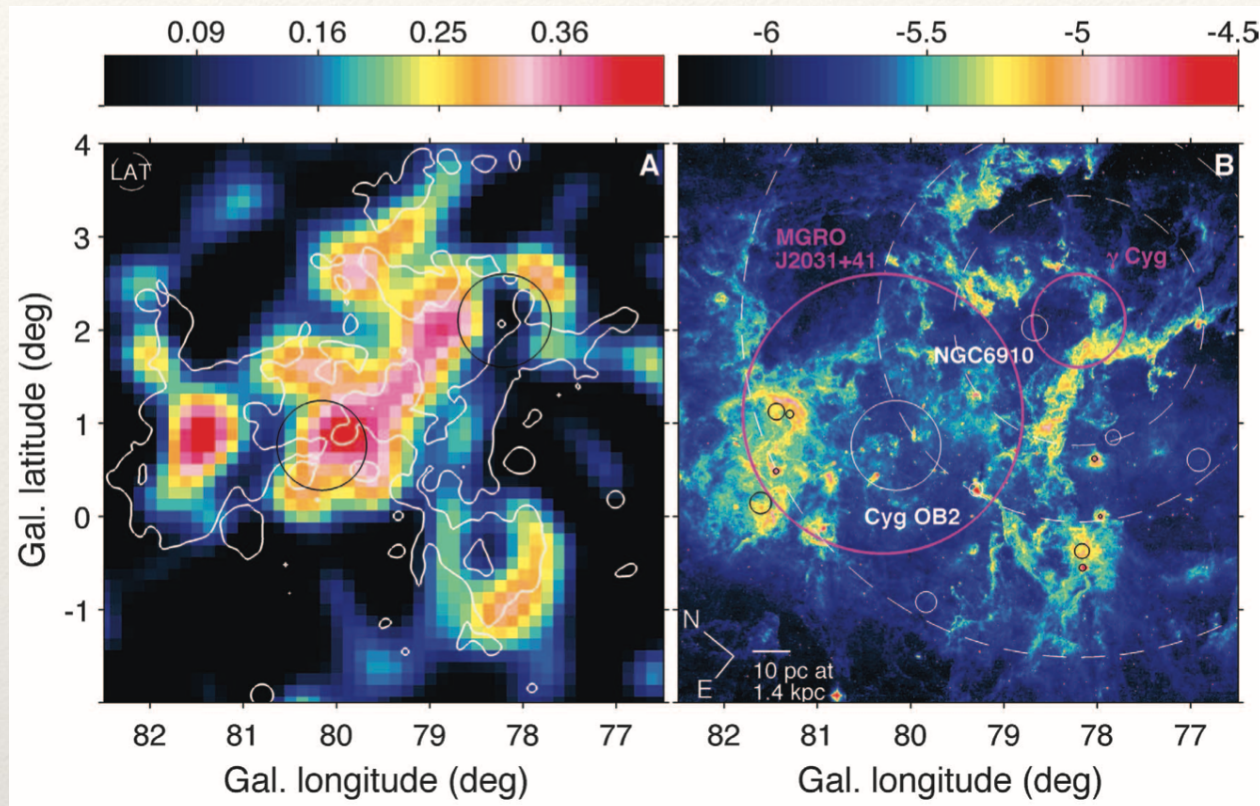
YSCs detected in gamma-rays

Recently several massive star clusters have been associated with gamma-ray sources

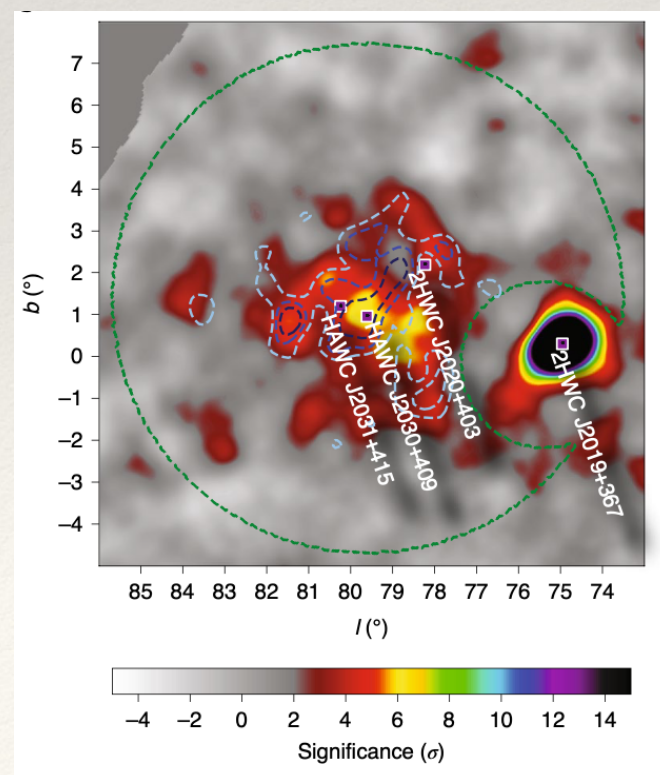
Name	$\log M/M_{\text{sun}}$	r_c/pc	D/kpc	age/Myr	$L_w/10^{38} \text{ erg s}^{-1}$	Reference
Westerlund 1	4.6 ± 0.045	1.5	4	4-6	10	Abramowski A., et al., 2012, A&A, 537, A114
Westerlund 2	4.56 ± 0.035	1.1	2.8 ± 0.4	1.5 - 2.5	2	Yang, de Oña Wilhelmi, Aharonian, 2018, A&A, 611 ,
Cyg. OB2	4.7 ± 0.3	5.2	1.4	3 - 6	2	Ackermann M., et al. 2011, Science , 334, 1103
NGC 3603	4.1 ± 0.10	1.1	6.9	2 - 3	?	Saha, L. et al 2020, ApJ, 897, 131
BDS 2003	4.39	0.2	4	1	?	Albert A., et al., 2020, arXiv:2012.15275
W40	2.5	0.44	0.44	1.5	?	Sun, X.-N. et al. 2020, A&A 639
RSGC 1	4.48	1.5	6.6	10 - 14	?	Sun et al. 2020, MNRAS 494
MC 20	~3	1.3	3.8 - 5.1	3 - 8	~4	Sun et al. 2021, A&A 659
NGC 6618		3.3	~2	< 3	?	Liu et al. 2022, MNRAS 513
30 Dor (LMC)	4.8-5.7	multiple	50	1	?	H. E. S. S. Collaboration et al., 2015, Science, 347, 406
NGC 2070/RCM 136	4.34-5	sub-clusters		5		

YSCs detected in gamma-rays

Cygnus Cocoon FermiLAT - Ackermann et al. (2011)

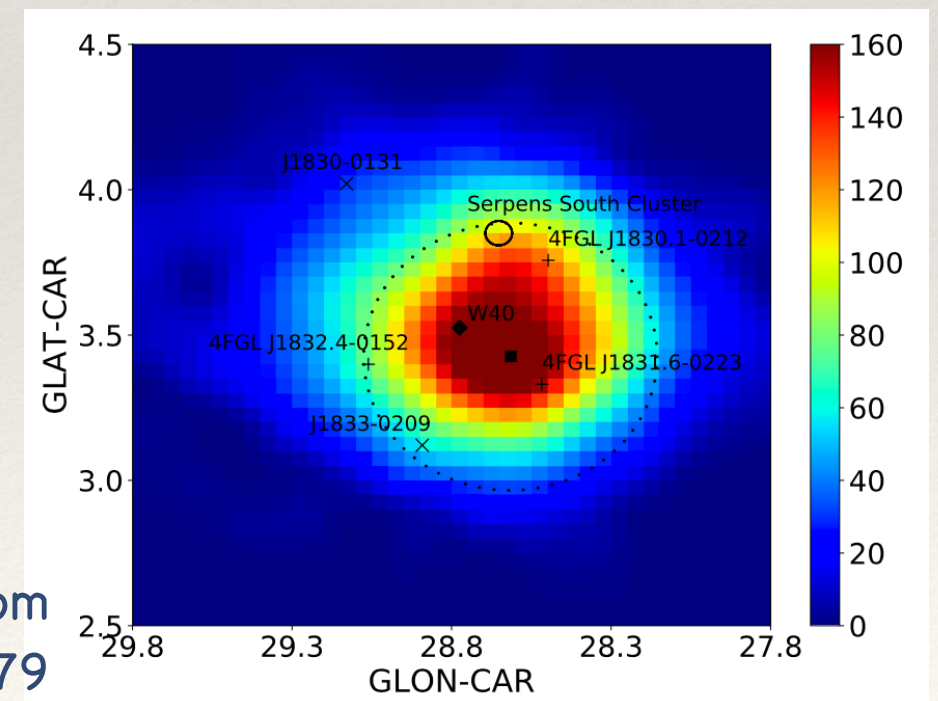


Westerlund 1
HESS coll. A&A (2022)



Cygnus Cocoon
HAWC coll. Nat. Astr.(2020)

W40 - FermiLAT data from
Sun et al. (2020) arxiv:2006.00879

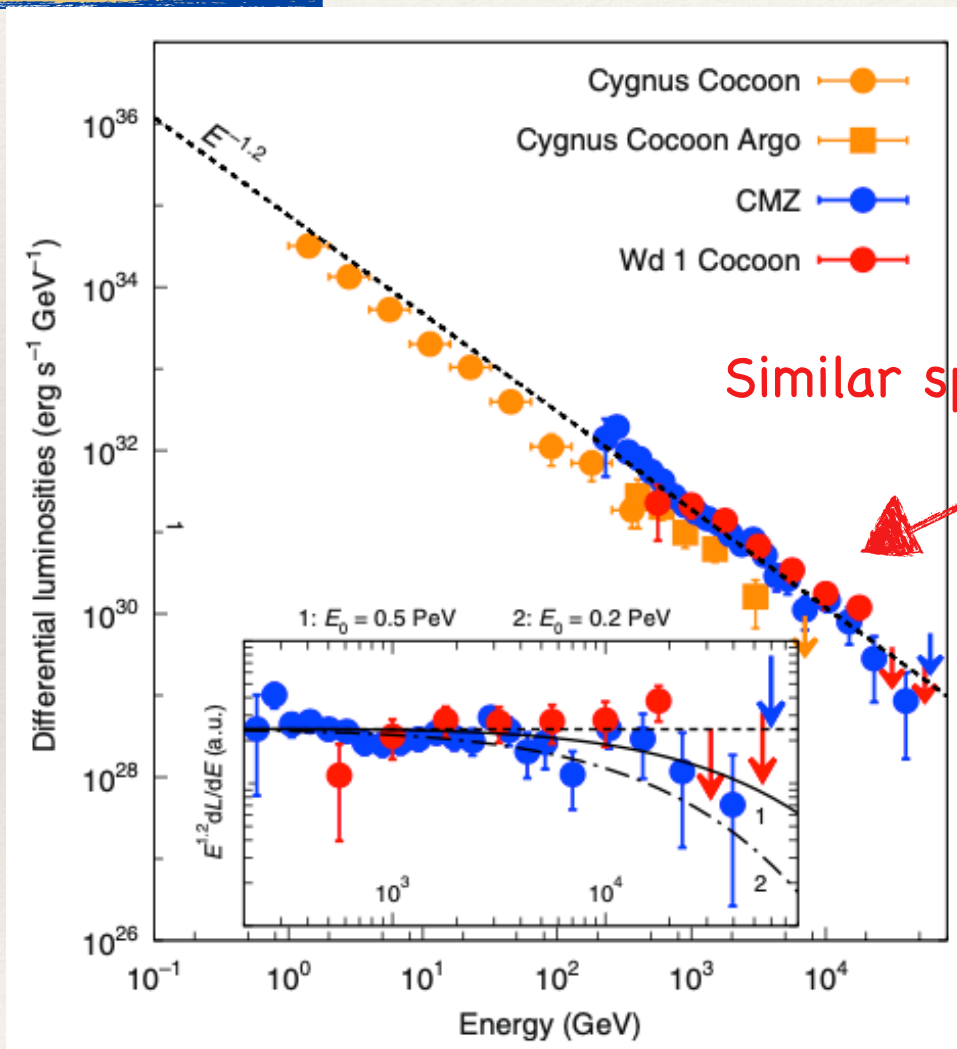


YSCs detected in gamma-rays

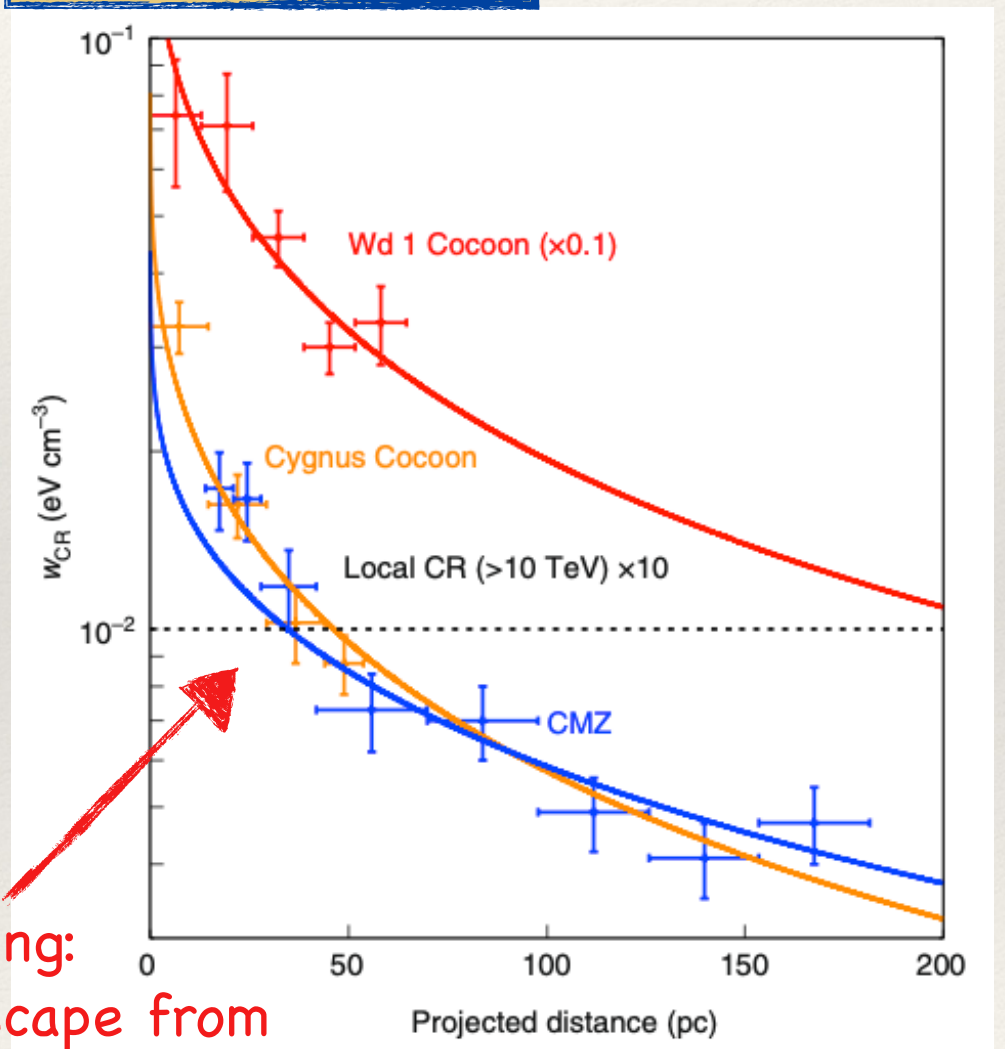
[Aharonian, Yang & Wilhelmi, Nat. Astr. (2019)]

Some clusters show similar spectra and radial profile

Spectrum



Radial CR profile

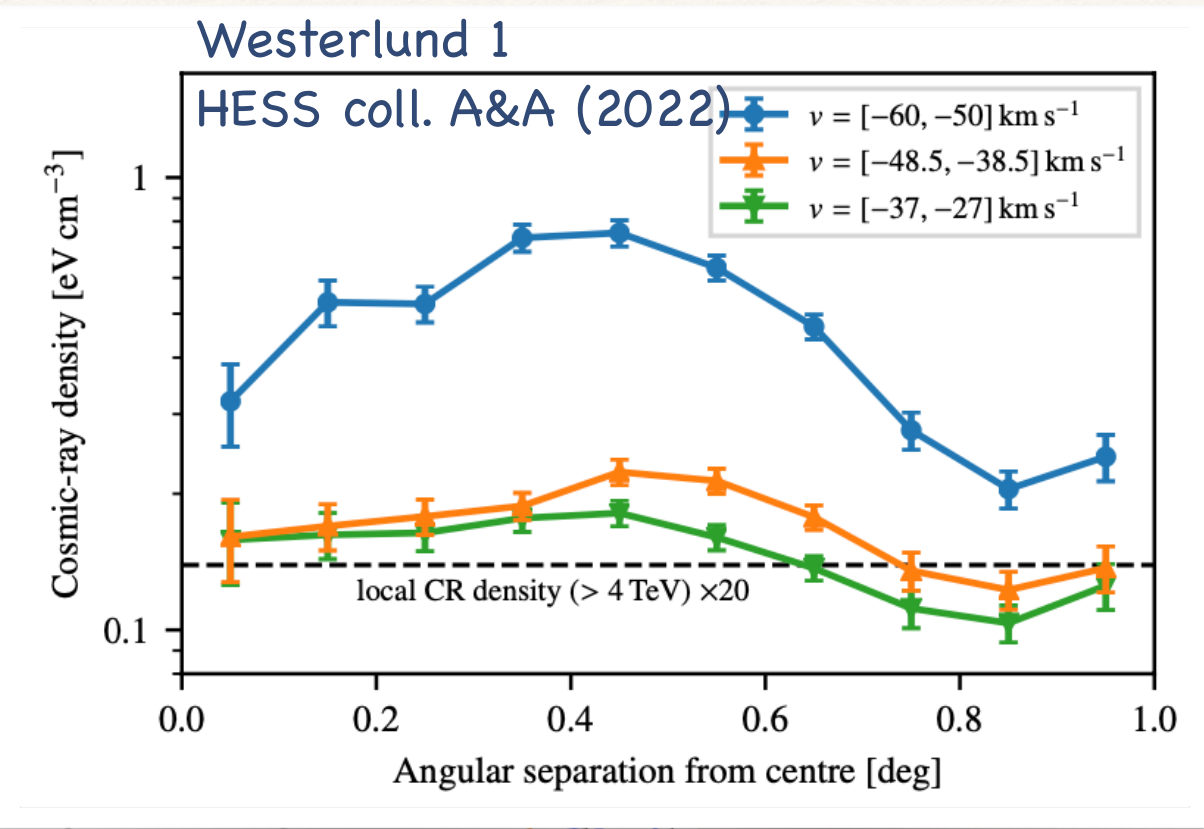
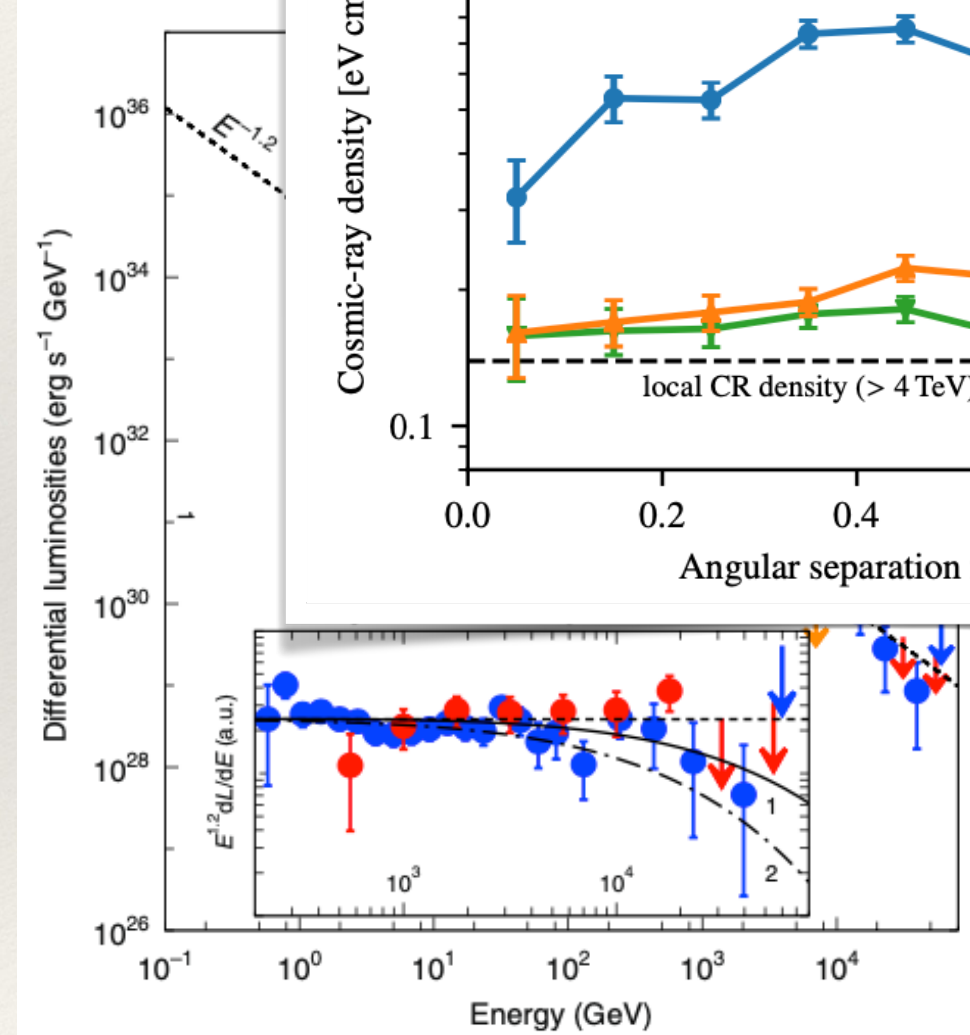


YSCs detected in gamma-rays

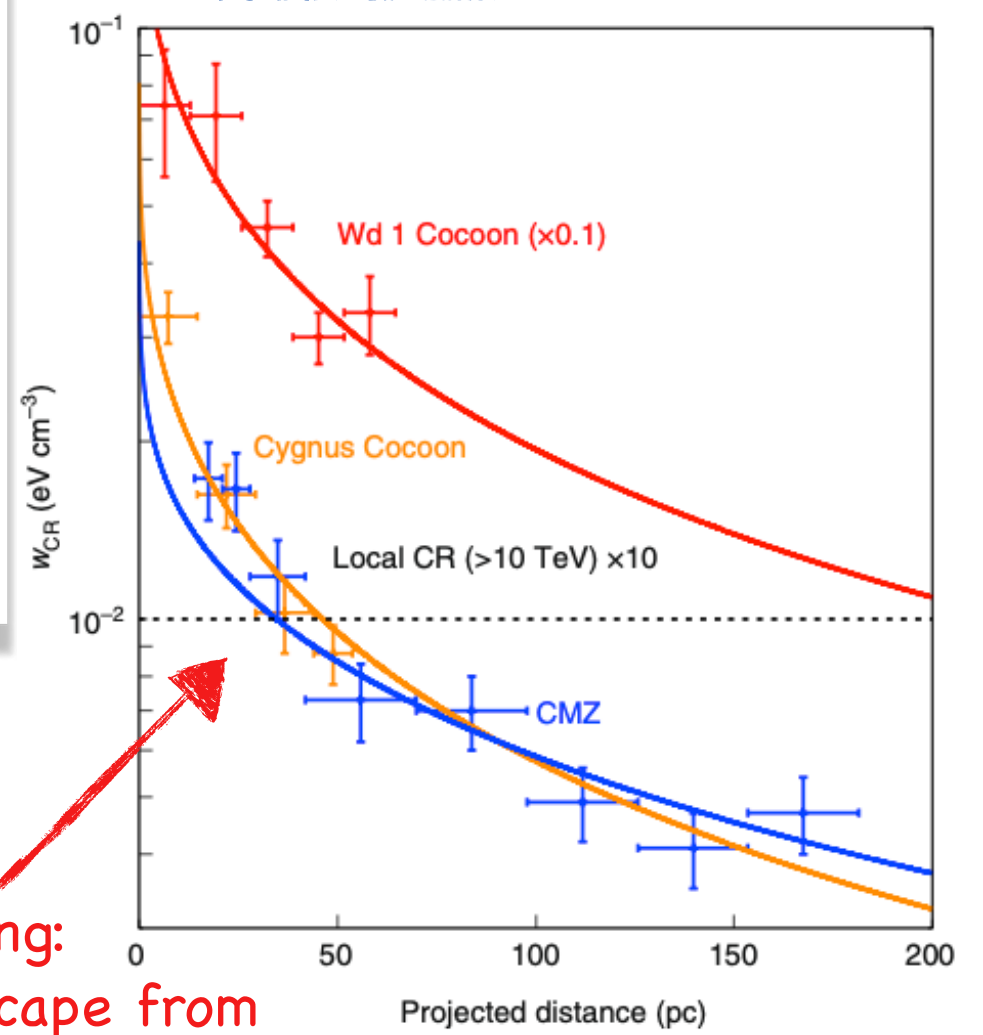
[Aharonian, Yang & Wilhelmi, Nat. Astr. (2019)]

Some clusters show similar spectra and radial profile

Spectrum



Radial CR profile



$1/r$ scaling:
CR diffusive escape from
continuous point source?

Energetics: stellar winds vs. SNe

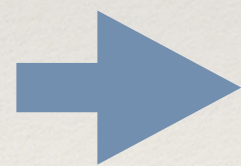
Salpeter (1955) initial mass function of stars: $f(M) = \frac{dN_{\text{star}}}{dM} \propto M^{-2.35}$

Power injected by SNe $P_{\text{SNe}} = 10^{51} \text{erg} \int_{8M_{\odot}}^{M_1} f(M) dM$

Power injected by winds $P_{\text{wind}} = \int_{M_{\text{min}}}^{M_{\text{max}}} \left[\frac{1}{2} \dot{M}_w(M) v_w(M)^2 \tau_{\text{life}}(M) \right] f(M) dM$

$v_w = 2.5 \sqrt{2G_N M/R}$ for line-driven winds;

\dot{M} from analytical (approximated) models [[Nieuwenhuijzen & de Jager\(1990\)](#)]



$$\frac{P_{\text{wind}}}{P_{\text{SNe}}} \simeq 0.1 \div 0.5$$

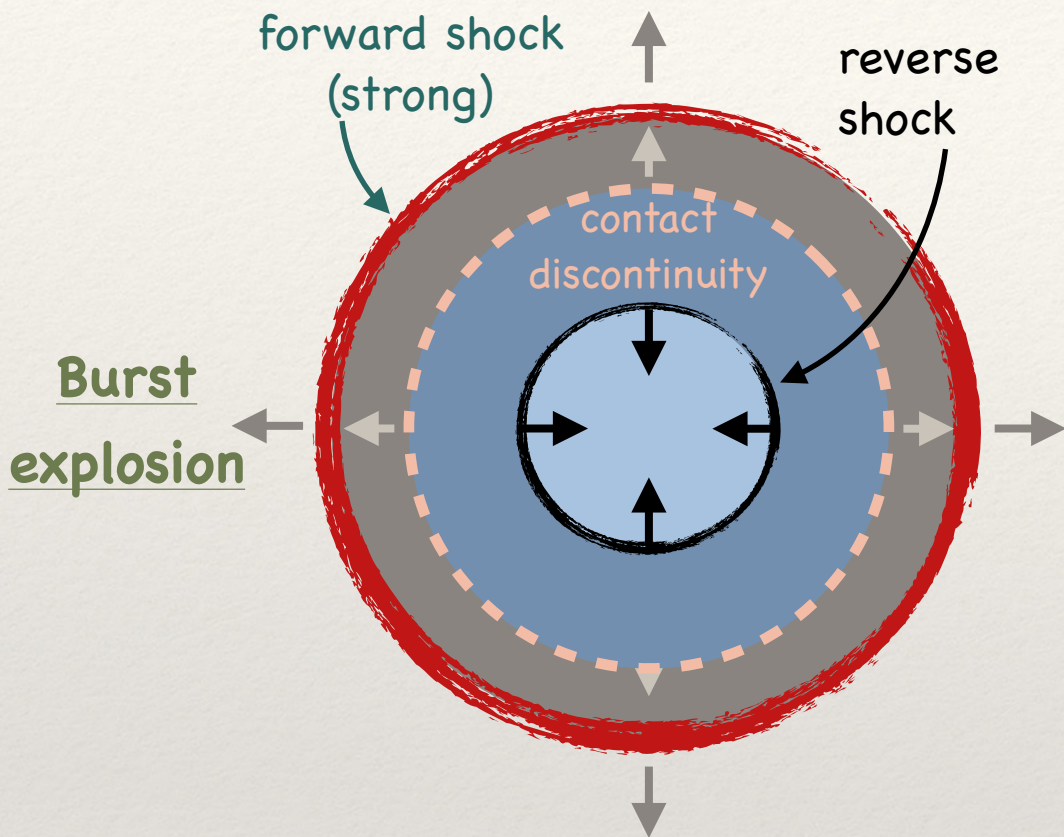
Uncertainty mainly due to mass loss rate

- Not accounting for WR stars
- Not accounting for failed supernovae $\sim 10\%$ of the total [[Adams et al. \(2017, MNRAS 469\)](#)]

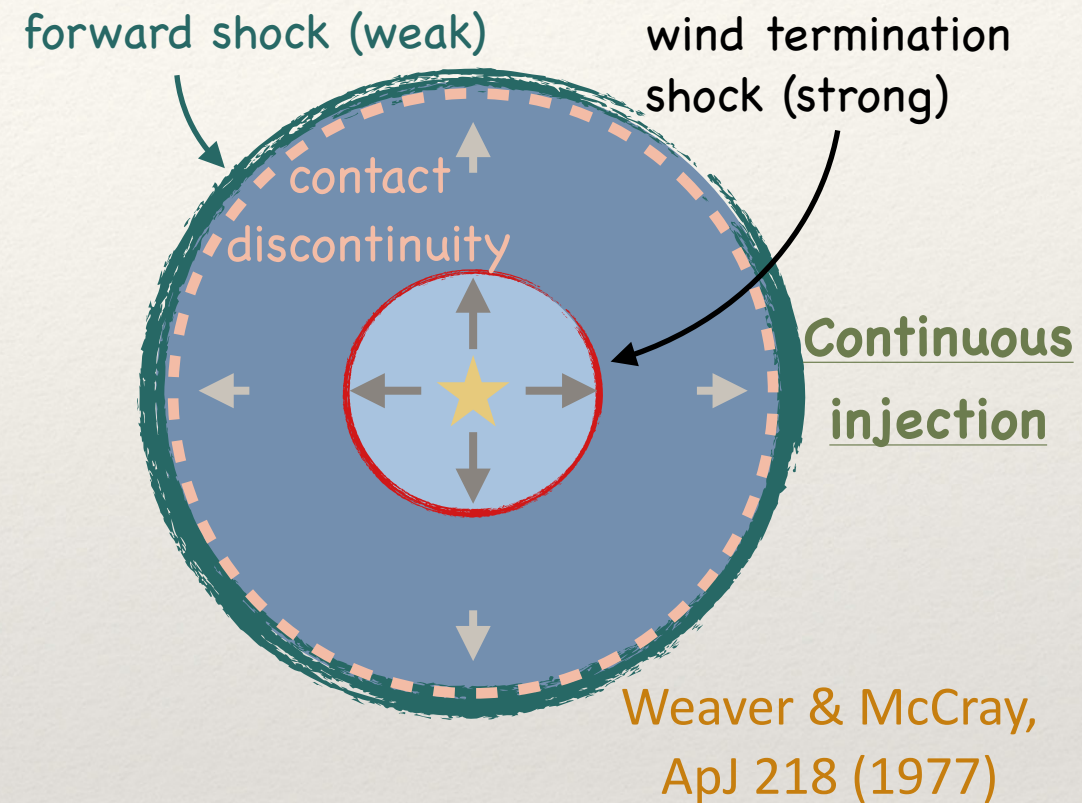
Stellar winds vs. SNRs

Cassé & Paul (1980, 1982) — Cesarsky & Montmerle (1983)

SNR

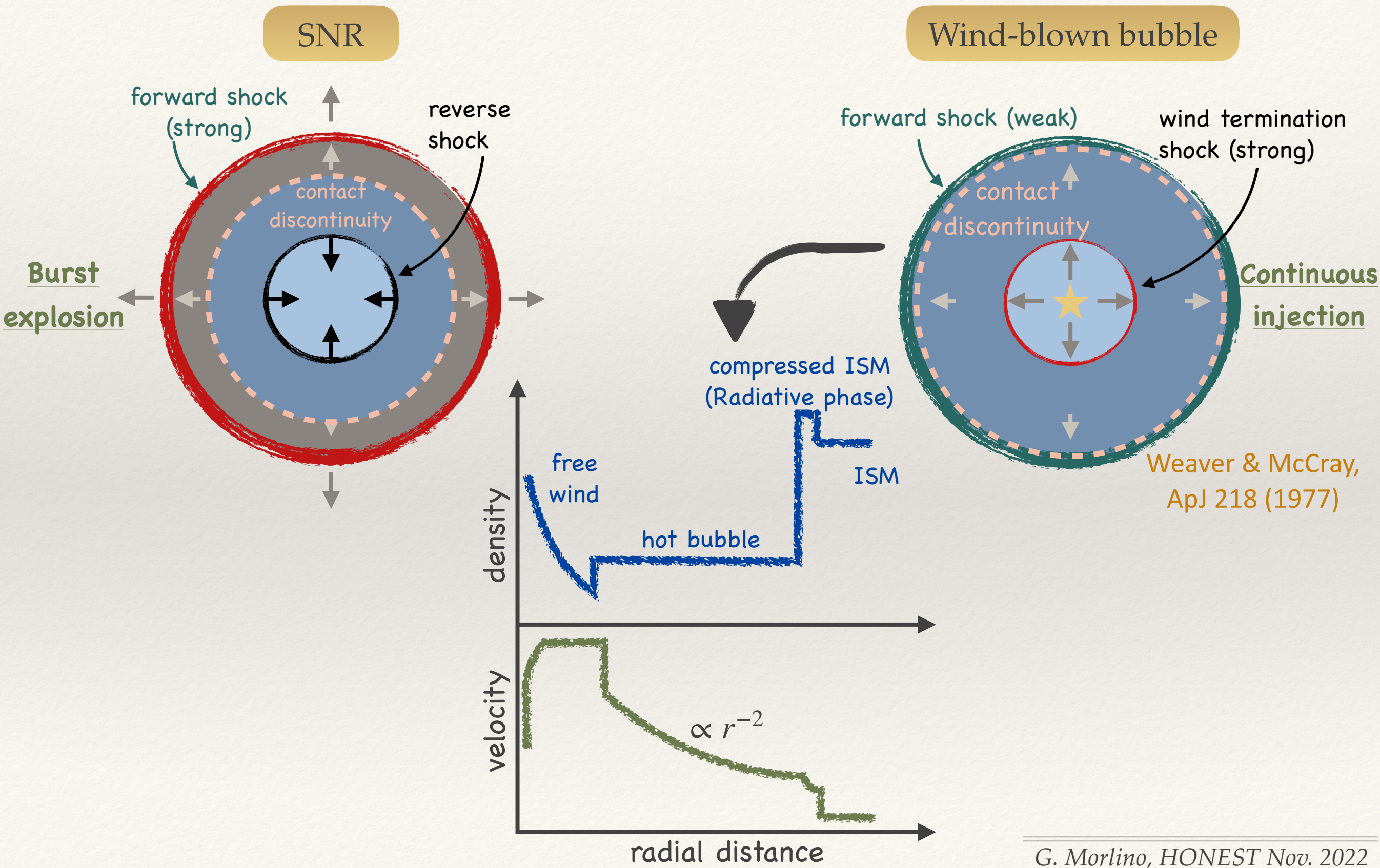


Wind-blown bubble



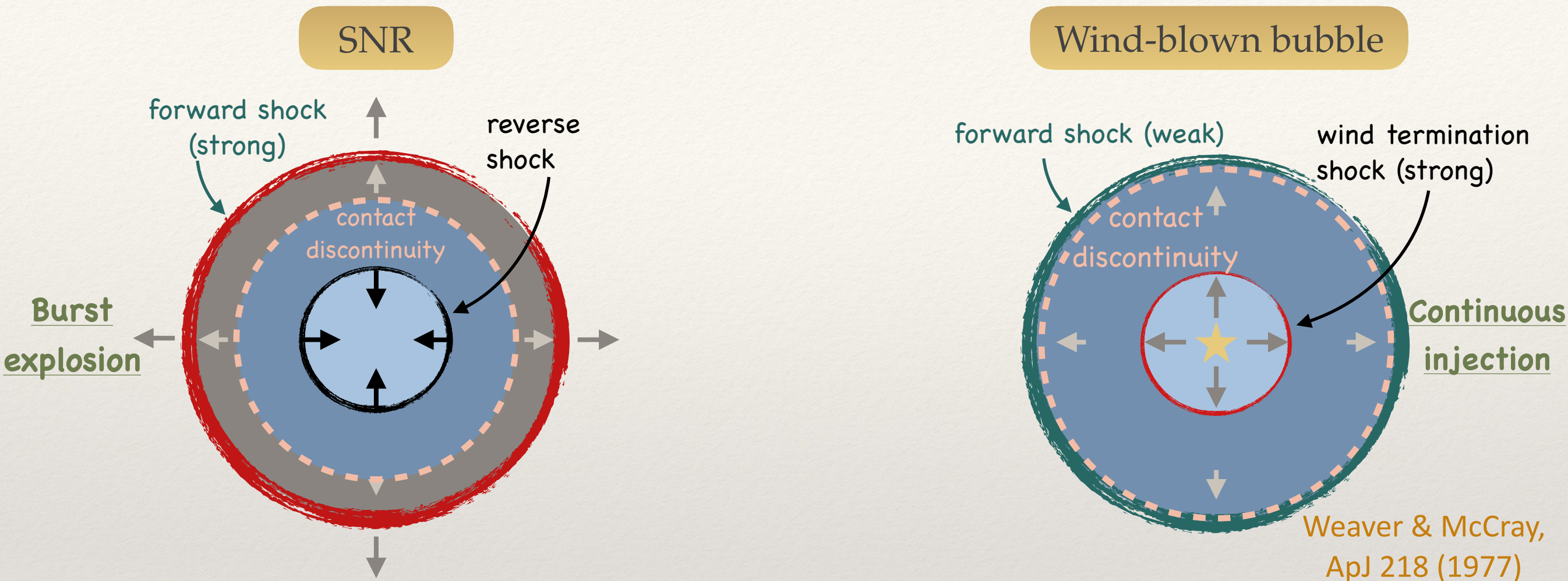
Stellar winds vs. SNRs

Cassé & Paul (1980, 1982) — Cesarsky & Montmerle (1983)



Stellar winds vs. SNRs

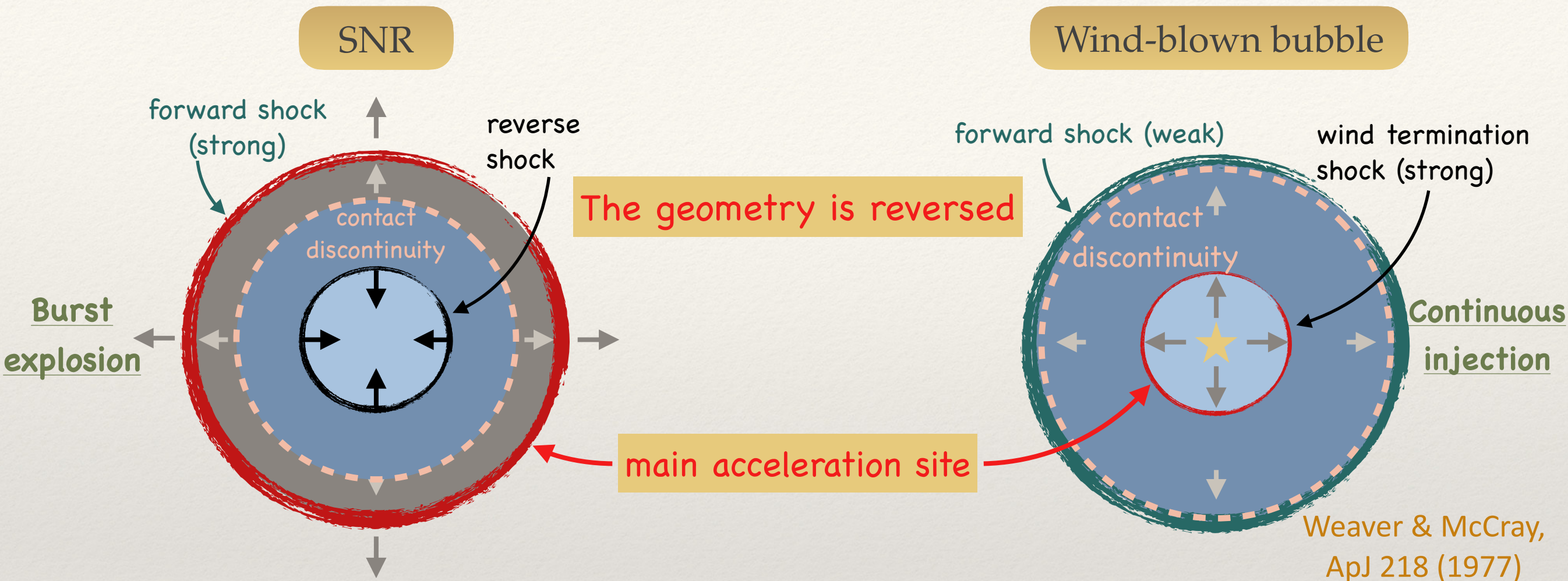
Cassé & Paul (1980, 1982) — Cesarsky & Montmerle (1983)



		Forward shock		Reverse shock	
	<i>age</i>	V_{FS} [km/s]	R_{FS} [pc]	V_{RS} [km/s]	R_{RS} [pc]
SNR	kyr	> 5000	< 1	< 3000	< 1
Wind bubble	Myr	10 - 20	50-100	< 3000	1-10

Stellar winds vs. SNRs

Cassé & Paul (1980, 1982) — Cesarsky & Montmerle (1983)



	age	Forward shock		Reverse shock	
		V_{FS} [km/s]	R_{FS} [pc]	V_{RS} [km/s]	R_{RS} [pc]
SNR	kyr	> 5000	< 1	< 3000	< 1
Wind bubble	Myr	10 - 20	50-100	< 3000	1-10

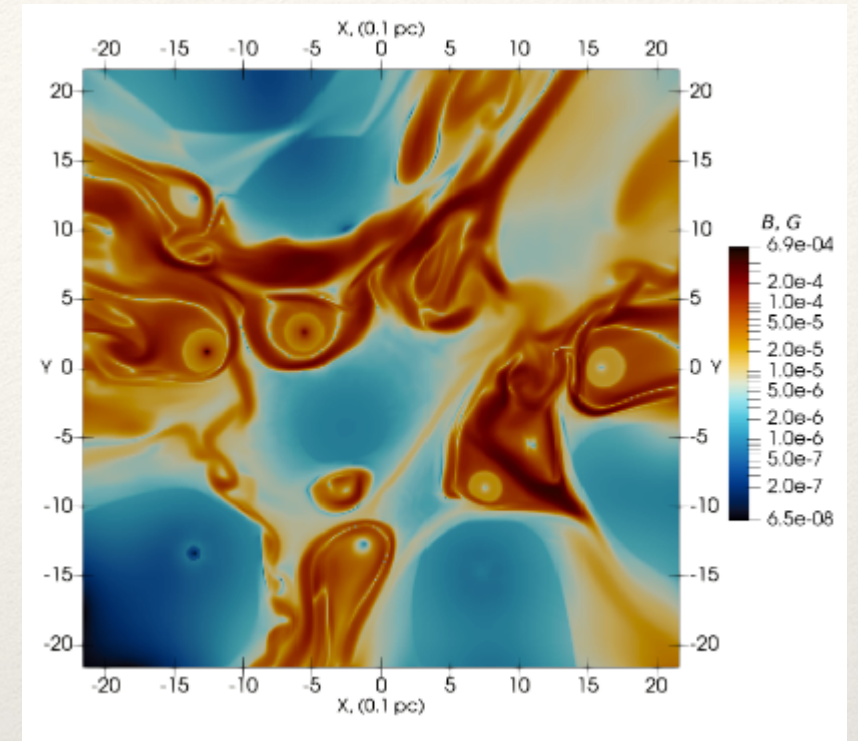
Magnetic field amplification

❖ MHD amplification

Wind-wind interaction results into MHD turbulence
(Inside the SC core $\sim 100 \mu\text{G}$ may be reached)

If we assume that a fraction η_B of kinetic energy is converted into magnetic field at the termination shock

$$\frac{\delta B^2}{4\pi} 4\pi r^2 v_w = \frac{1}{2} \eta_B \dot{M} v_w^2 \Rightarrow \delta B(R_s) \simeq 4 \mu\text{G} \left(\frac{\eta_B}{0.05} \right)^{\frac{1}{2}} \left(\frac{\dot{M}}{10^{-4} M_\odot/\text{yr}} \right)^{\frac{3}{10}} \left(\frac{v_w}{2500 \text{ km/s}} \right)^{\frac{1}{10}} \quad \text{Badmaev et al. (2022)}$$



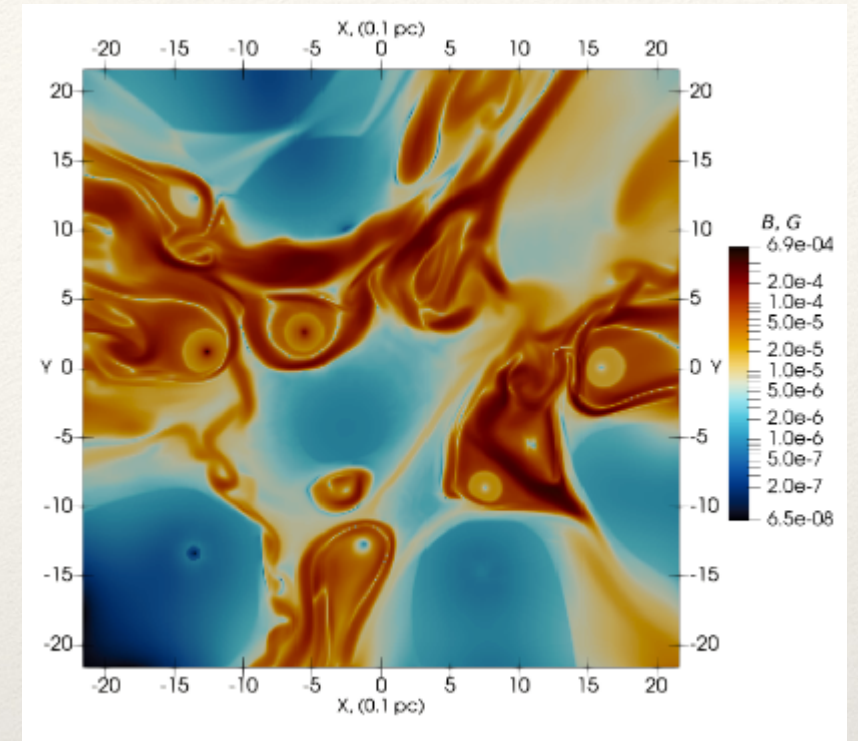
Magnetic field amplification

❖ MHD amplification

Wind-wind interaction results into MHD turbulence
(Inside the SC core $\sim 100 \mu\text{G}$ may be reached)

If we assume that a fraction η_B of kinetic energy is converted into magnetic field at the termination shock

$$\frac{\delta B^2}{4\pi} 4\pi r^2 v_w = \frac{1}{2} \eta_B \dot{M} v_w^2 \Rightarrow \delta B(R_s) \simeq 4 \mu\text{G} \left(\frac{\eta_B}{0.05} \right)^{\frac{1}{2}} \left(\frac{\dot{M}}{10^{-4} M_\odot/\text{yr}} \right)^{\frac{3}{10}} \left(\frac{v_w}{2500 \text{ km/s}} \right)^{\frac{1}{10}} \quad \text{Badmaev et al. (2022)}$$



❖ CR self-amplification

In the linear regime:

$$\mathcal{F}_0(k) = \frac{\pi}{2} \frac{\xi_{\text{CR}}}{\Lambda_p} \frac{v_{\text{sh}}}{v_A} = \frac{\pi}{2} \frac{\xi_{\text{CR}}}{\Lambda_p} \eta_b^{-1/2} \simeq 0.06 \frac{\xi_{\text{CR}}}{0.1} \left(\frac{\eta_B}{0.05} \right)^{-1/2}$$

Self-amplification may be relevant at low energies

Maximum energy: first order estimate

Hillas criterium

$$E_{\max} \sim \left(\frac{q}{c} \right) B_{\text{sh}} u_{\text{sh}} R_{\text{sh}}$$

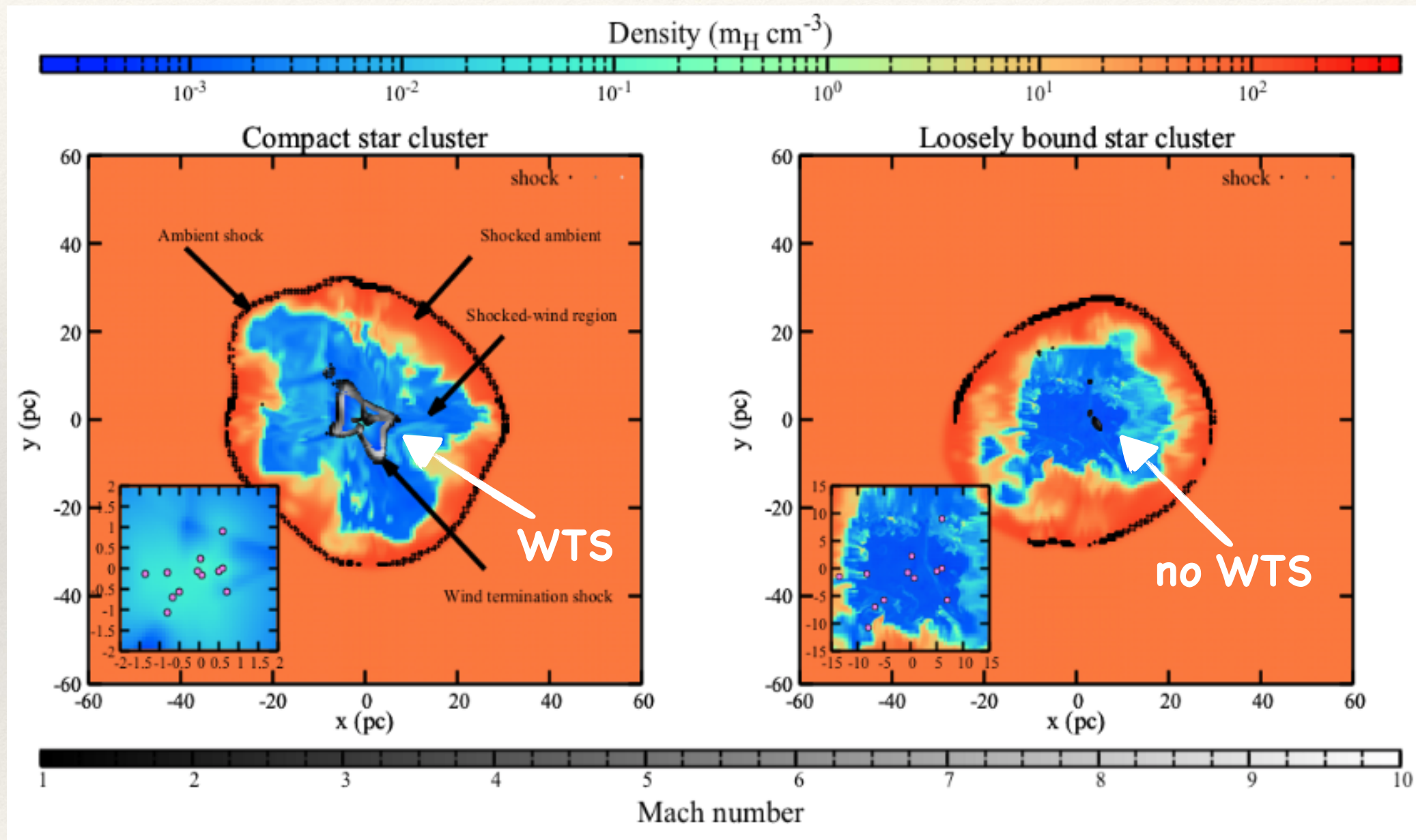
	dM/dt M_{sol}/yr	u_{sh} km/s	R_{sh} pc	B μG	age yr	lim E_{\max}	E_{\max} TeV
SNR	—	> 5000	< 1	~100 self-amplification	~10 ³	time limited	~10-100
WTS (single star)	10 ⁻⁶	< 3000	~ 1	~ 1 MHD turbulence	~10 ⁶	space limited	~ 10
WTS (massive cluster)	10 ⁻⁴	< 3000	> 10	> 10 MHD turbulence	~10 ⁶	space limited	~> 1000

For massive star cluster ($\gtrsim 10^4 M_{\odot}$) PeV energies can be reached

Cluster compactness

[Gupta, Nath, Sharma & Eichler, MNRAS 2020]

A WTS is generated if the cluster is compact enough, such that $R_{\text{cluster}} \ll R_{\text{ts}}$



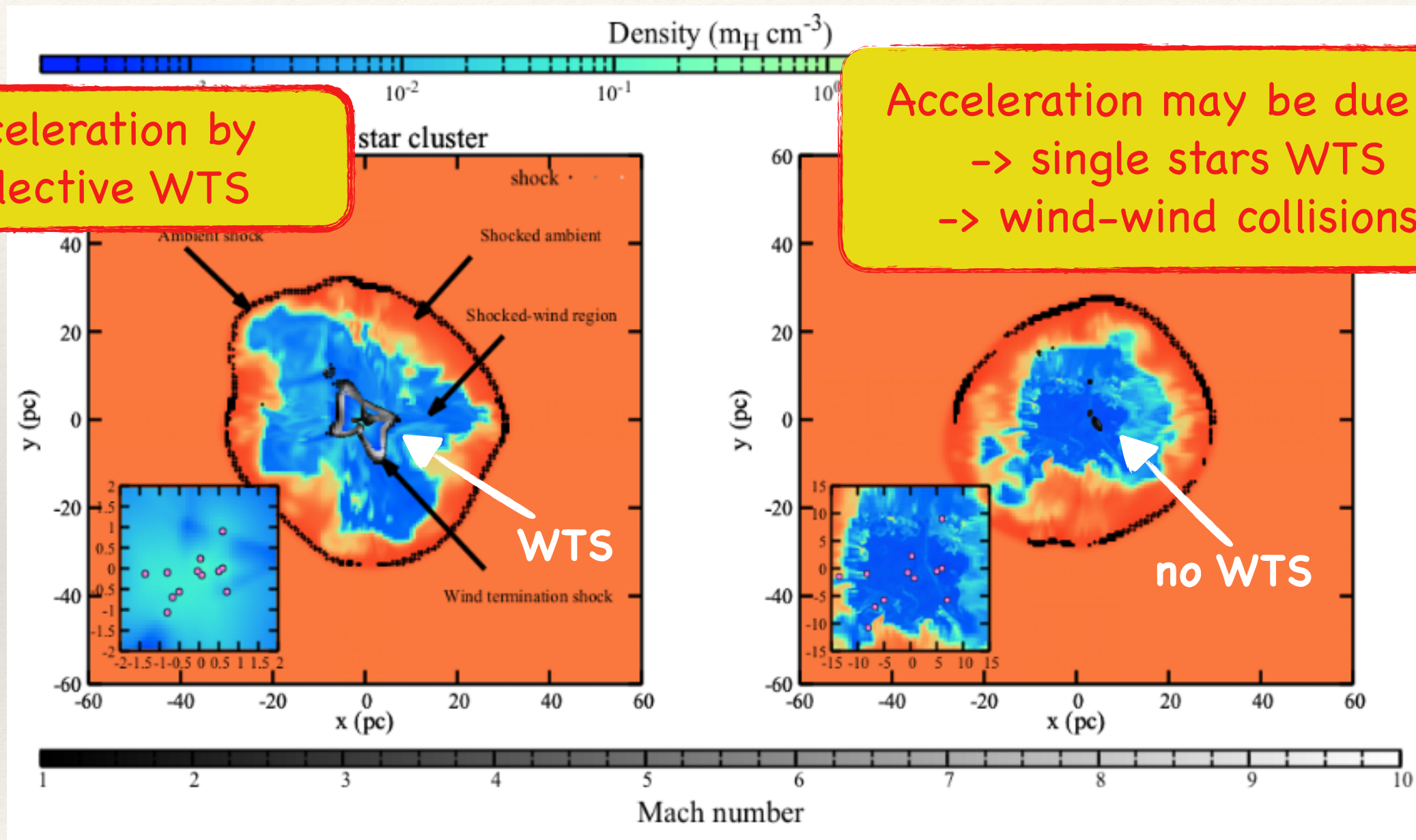
Compact cluster

Loose cluster

Cluster compactness

[Gupta, Nath, Sharma & Eichler, MNRAS 2020]

A WTS is generated if the cluster is compact enough, such that $R_{\text{cluster}} \ll R_{\text{ts}}$



Acceleration by collective WTS

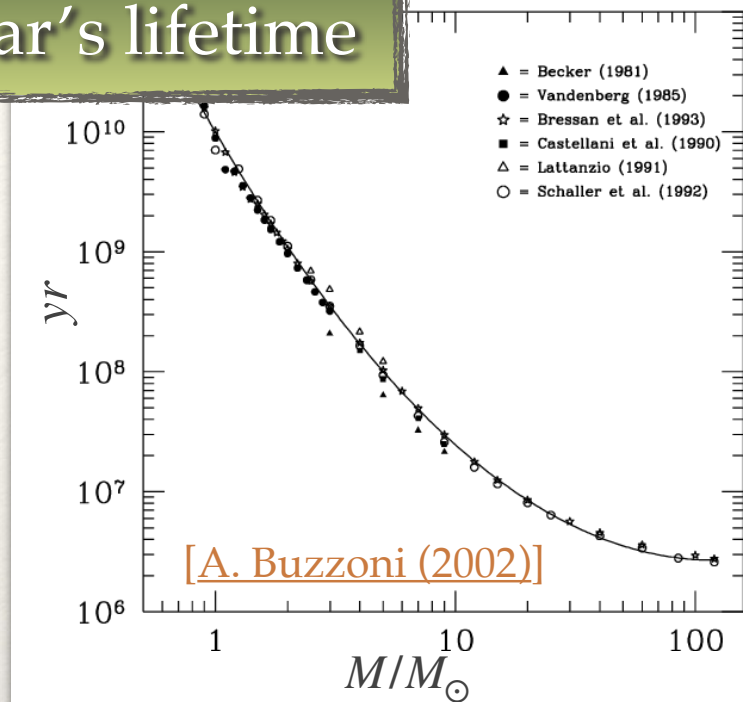
Acceleration may be due to
-> single stars WTS
-> wind-wind collisions

Compact cluster

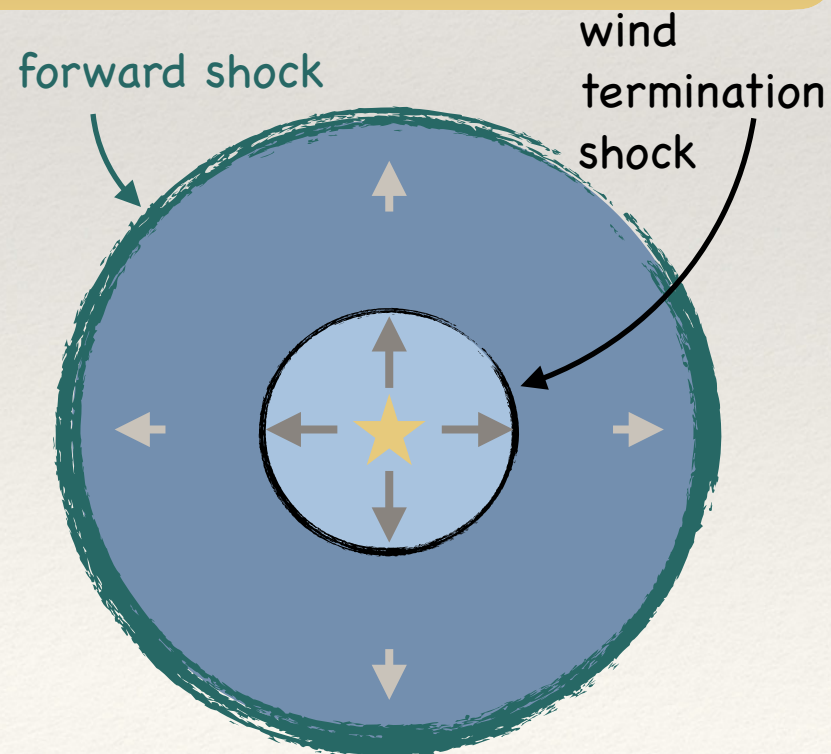
Loose cluster

Young vs. old clusters

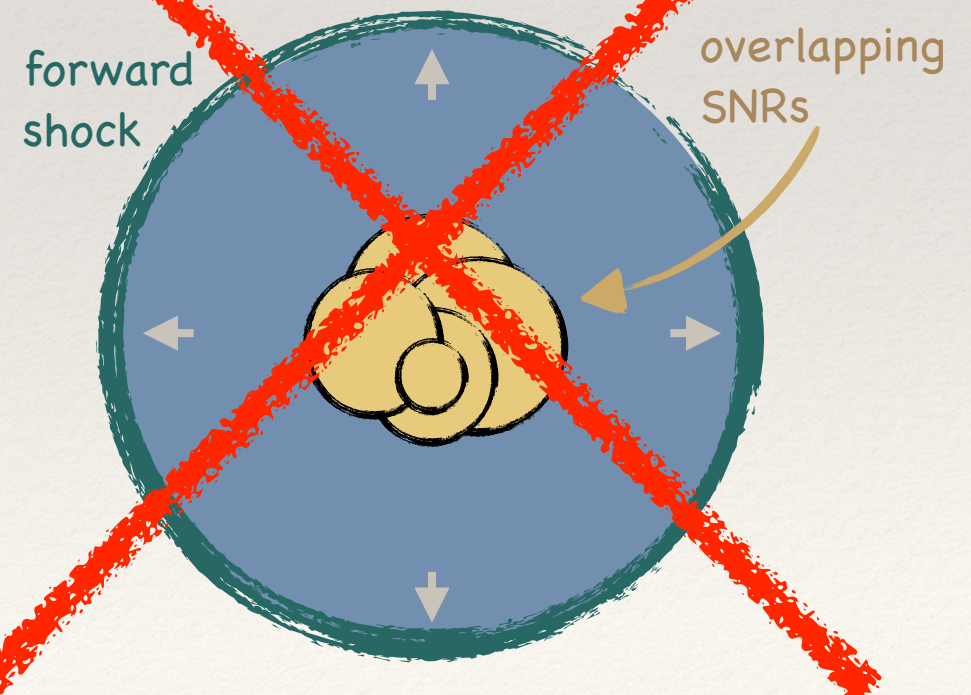
Star's lifetime



$t \lesssim 3 \text{ Myr}$ only stellar wind



~~$t \gtrsim 3 \text{ Myr}$ stellar wind + SNe~~

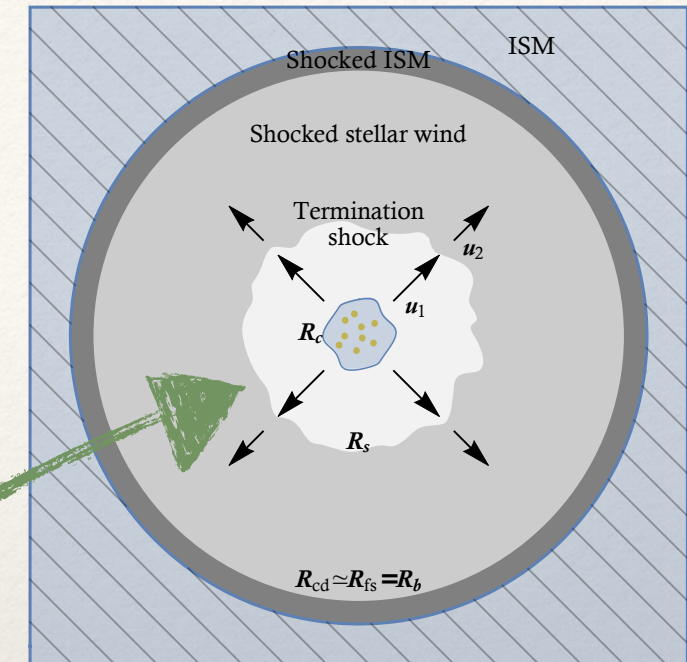


Particle acceleration at the wind TS

GM, Blasi, Peretti & Cristofari (2019)

Time-stationary transport equation in spherical geometry:

$$\frac{\partial}{\partial r} \left[r^2 D(r, p) \frac{\partial f}{\partial r} \right] - r^2 u(r) \frac{\partial f}{\partial r} + \frac{d[r^2 u]}{dr} \frac{p}{3} \frac{\partial f}{\partial p} + r^2 Q(r, p) = 0$$



- Injection only at the termination shock: $Q(r, p) \propto \delta(p - p_{\text{inj}}) \delta(r - R_s)$

- Wind velocity profile:
$$u(r) = \begin{cases} u_1 = v_w & \text{for } r < R_s, \\ \frac{u_1}{\sigma} \left(\frac{R_s}{r} \right)^2 & \text{for } R_s < r < R_b, \\ 0 & \text{for } r > R_b; \end{cases}$$

- Boundary conditions:

1. No net flux at the cluster center: $r^2 [D \partial_r f - u f]_{r=R_c} = 0$
2. Matching the Galactic distribution: $f(r \rightarrow \infty, p) = f_{\text{gal}}(p)$

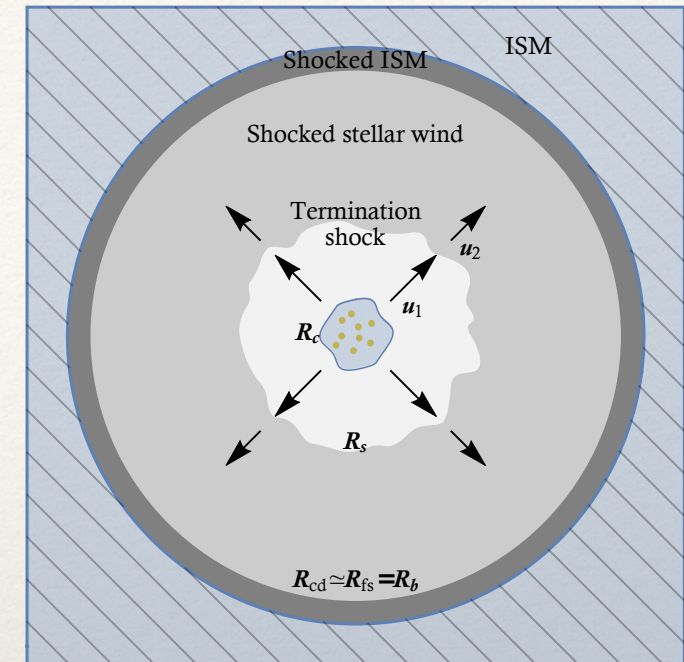
Particle acceleration at the wind TS

GM, Blasi, Peretti & Cristofari (2019)

Time-stationary transport equation in spherical geometry:

$$\frac{\partial}{\partial r} \left[r^2 D(r, p) \frac{\partial f}{\partial r} \right] - r^2 u(r) \frac{\partial f}{\partial r} + \frac{d[r^2 u]}{dr} \frac{p}{3} \frac{\partial f}{\partial p} + r^2 Q(r, p) = 0$$

- Arbitrary diffusion coefficient: $D(r, p)$



Wind-wind collision and non-stationarity can produce high level of HD turbulence

Assuming that a fraction $\eta_B \gtrsim 1\%$ of kinetic wind energy is converted into magnetic energy $\frac{\delta B}{4\pi} 4\pi r^2 v_w = \frac{1}{2} \eta_B \dot{M} v_w^2 \Rightarrow \delta B(R_s) \gtrsim \mu G$

The type of turbulent cascade can result into different diffusion coefficients

$$\begin{cases} D_{\text{Kol}}(E) = \frac{v}{3} r_L (\delta B)^{1/3} L_c^{2/3} \\ D_{\text{Kra}}(E) = \frac{v}{3} r_L (\delta B)^{1/2} L_c^{1/2} \\ D_{\text{Bohm}}(E) = \frac{v}{3} r_L (\delta B) \end{cases}$$

$L_c \sim \text{pc}$ is the injection scale of turbulence

Maximum energy: a more detailed analysis

GM, Blasi, Peretti & Cristofari (2019)

Solution of diffusive shock acceleration in spherical geometry

$$f_s(p) = s \frac{\eta_{\text{inj}} n_1}{4\pi p_{\text{inj}}^3} \left(\frac{p}{p_{\text{inj}}} \right)^{-s} e^{-\Gamma_1(p)} e^{-\Gamma_2(p)}$$

Maximum energy: a more detailed analysis

GM, Blasi, Peretti & Cristofari (2019)

Solution of diffusive shock acceleration in spherical geometry

Standard power-law
for plane shocks

$$s = \frac{3u_1}{u_1 - u_2}$$

$$f_s(p) = s \frac{\eta_{\text{inj}} n_1}{4\pi p_{\text{inj}}^3} \left(\frac{p}{p_{\text{inj}}} \right)^{-s} e^{-\Gamma_1(p)} e^{-\Gamma_2(p)}$$

Maximum energy: a more detailed analysis

GM, Blasi, Peretti & Cristofari (2019)

Solution of diffusive shock acceleration in spherical geometry

Standard power-law
for plane shocks

$$s = \frac{3u_1}{u_1 - u_2}$$

$$f_s(p) = s \frac{\eta_{\text{inj}} n_1}{4\pi p_{\text{inj}}^3} \left(\frac{p}{p_{\text{inj}}} \right)^{-s} e^{-\Gamma_1(p)} e^{-\Gamma_2(p)}$$

Maximum energy due to confinement in the upstream:
the effective plasma speed decreased reducing the energy gain

Maximum energy: a more detailed analysis

GM, Blasi, Peretti & Cristofari (2019)

Solution of diffusive shock acceleration in spherical geometry

Standard power-law
for plane shocks

$$s = \frac{3u_1}{u_1 - u_2}$$

$$f_s(p) = s \frac{\eta_{\text{inj}} n_1}{4\pi p_{\text{inj}}^3} \left(\frac{p}{p_{\text{inj}}} \right)^{-s} e^{-\Gamma_1(p)} e^{-\Gamma_2(p)}$$

Maximum energy due
to escaping from
the downstream

Maximum energy due to confinement in the upstream:
the effective plasma speed decreased reducing the energy gain

Maximum energy: a more detailed analysis

GM, Blasi, Peretti & Cristofari (2019)

Solution of diffusive shock acceleration in spherical geometry

Standard power-law for plane shocks

$$s = \frac{3u_1}{u_1 - u_2}$$

$$f_s(p) = \frac{\eta_{\text{inj}} n_1}{4\pi p_{\text{inj}}^3} \left(\frac{p}{p_{\text{inj}}} \right)^{-s} e^{-\Gamma_1(p)} e^{-\Gamma_2(p)}$$

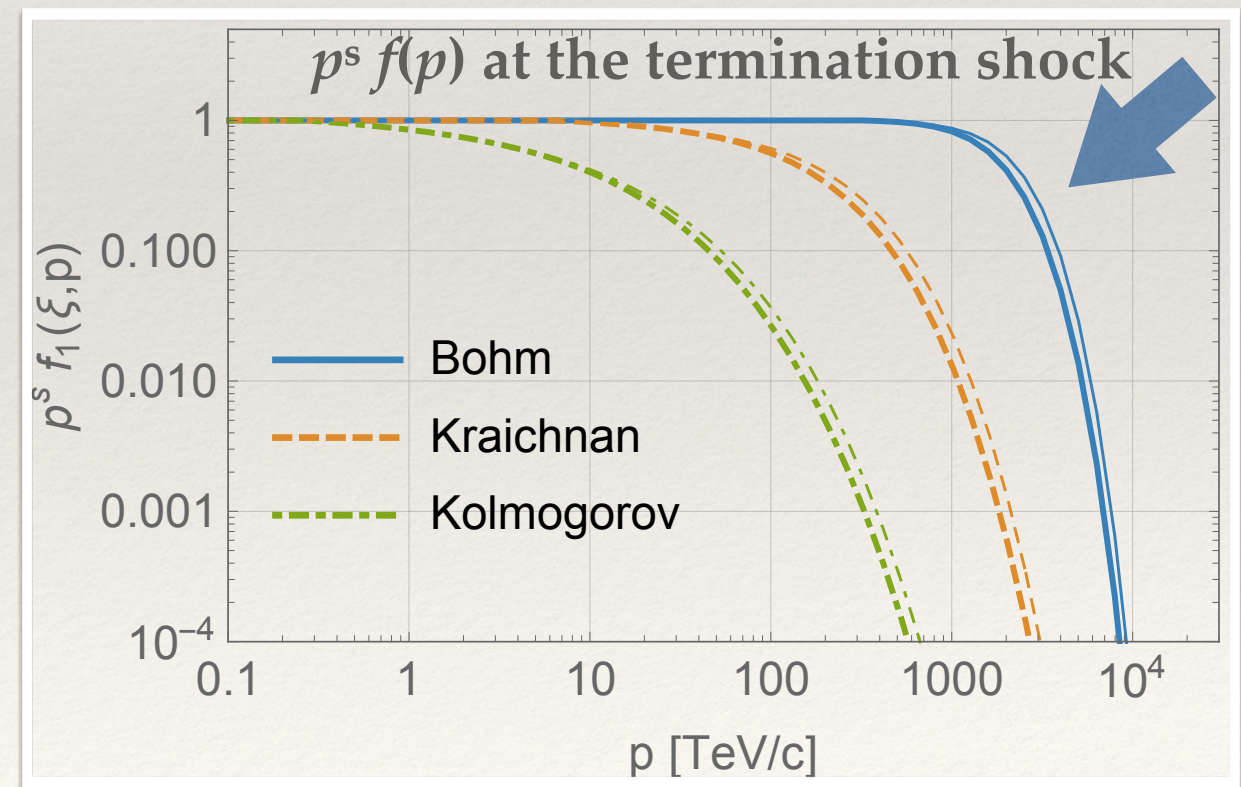
Maximum energy due to escaping from the downstream

Maximum energy due to confinement in the upstream: the effective plasma speed decreased reducing the energy gain

The diffusion coefficient has a strong impact on the cutoff shape and effective maximum energy

Typical values for massive stellar clusters

$$\begin{cases} \dot{M} = 10^{-4} M_{\odot} \text{ yr}^{-1} \\ v_w = 3000 \text{ km/s} \\ L_{\text{CR}} = 0.1 L_w \\ \eta_B = 0.01 \end{cases}$$



Maximum energy: a more detailed analysis

GM, Blasi, Peretti & Cristofari (2019)

Solution of diffusive shock acceleration in spherical geometry

Standard power-law for plane shocks

$$s = \frac{3u_1}{u_1 - u_2}$$

$$f_s(p) = \frac{\eta_{\text{inj}} n_1}{4\pi p_{\text{inj}}^3} \left(\frac{p}{p_{\text{inj}}} \right)^{-s} e^{-\Gamma_1(p)} e^{-\Gamma_2(p)}$$

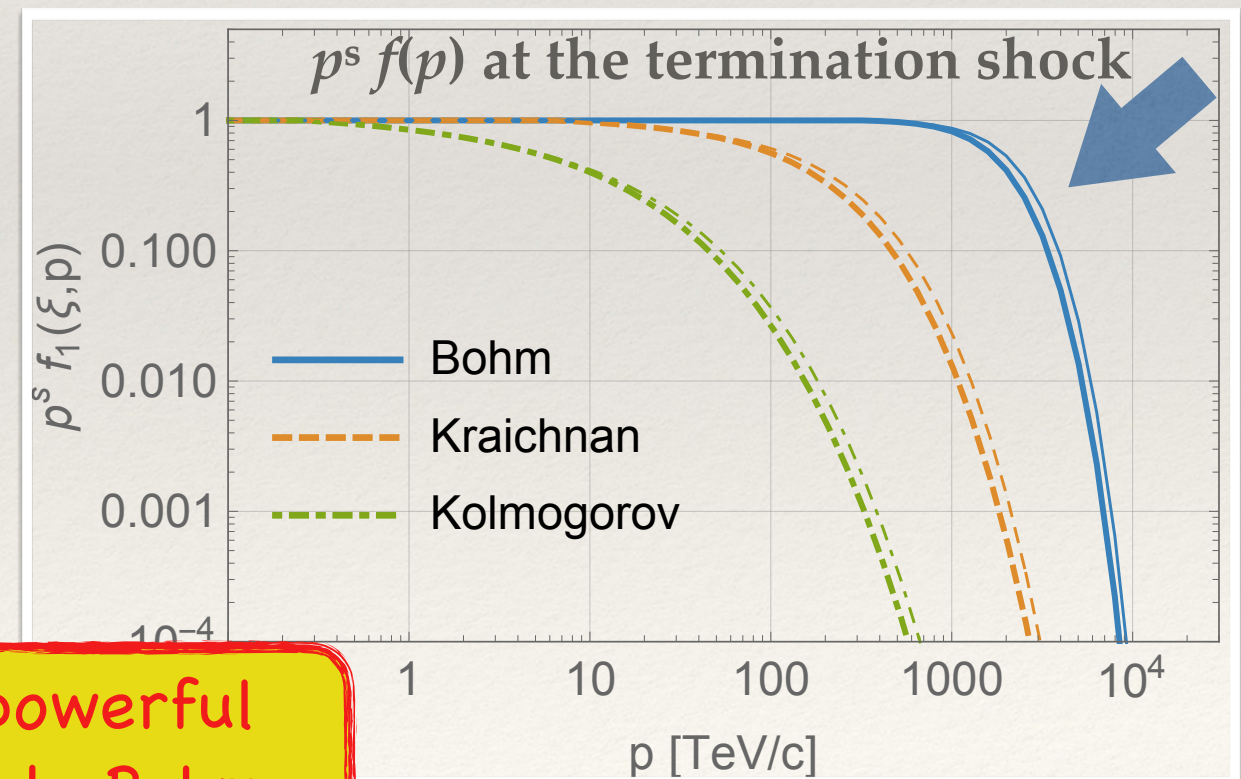
Maximum energy due to escaping from the downstream

Maximum energy due to confinement in the upstream: the effective plasma speed decreased reducing the energy gain

The diffusion coefficient has a strong impact on the cutoff shape and effective maximum energy

Typical values for massive stellar clusters

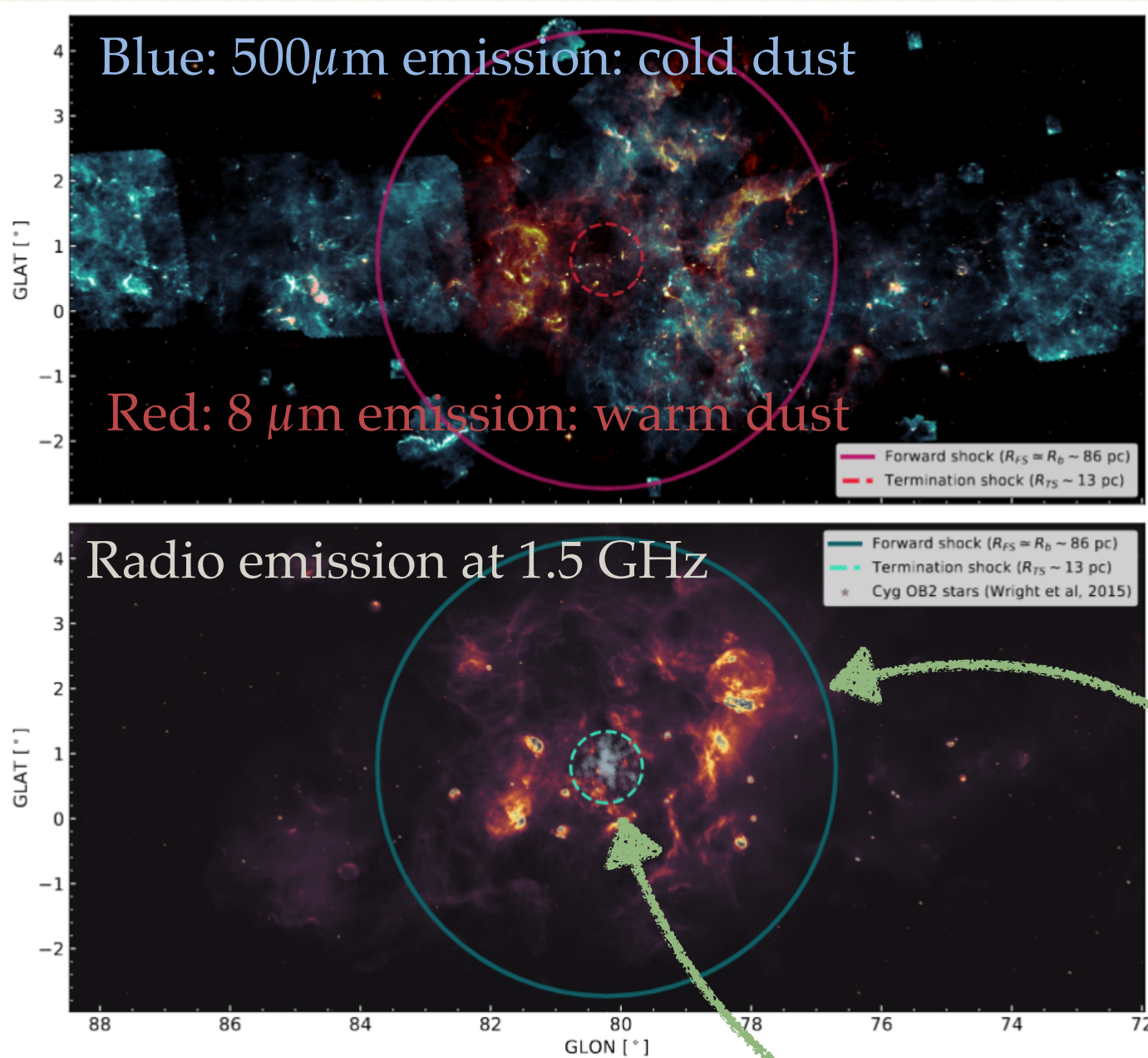
$$\begin{cases} \dot{M} = 10^{-4} M_{\odot} \text{ yr}^{-1} \\ v_w = 3000 \text{ km/s} \\ L_{\text{CR}} = 0.1 L_w \\ \eta_B = 0.01 \end{cases}$$



PeV energies can be reached in very powerful stellar clusters if the diffusion is close to Bohm

The case of Cygnus Cocoon

[S. Menchiari et al. in preparation]



Assumed properties

- ❖ Wind luminosity $\simeq 2 \times 10^{38}\text{ erg s}^{-1}$
- ❖ Ejecta mass $\dot{M} \simeq 10^{-4}M_{\odot}\text{ yr}^{-1}$;
- ❖ wind speed $v_w \simeq 2300\text{ km s}^{-1}$
- ❖ Cluster age $\simeq 3\text{ Myr}$
- ❖ Average ISM density $\simeq 10\text{ cm}^{-3}$

Estimated size of the bubble $\simeq 90\text{ pc}$

Termination shock radius $\simeq 13\text{ pc}$

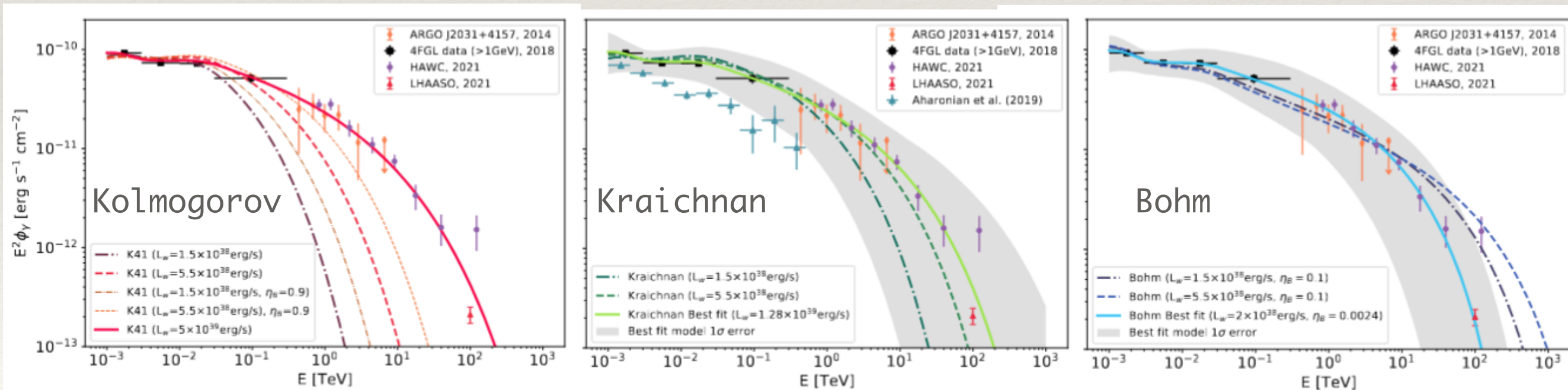
The case of Cygnus Cocoon

[S. Menchiari et al. in preparation]

Model	Kolmogorov	Kraichnan	Bohm
Wind luminosity	$5 \times 10^{39} \text{ erg s}^{-1}$	$1.3 \times 10^{39} \text{ erg s}^{-1}$	$2 \times 10^{37} \text{ erg s}^{-1}$
Magnetic field	$35 \mu\text{G}$	$20 \mu\text{G}$	$5 \mu\text{G}$
Acc. efficiency	0.4%	0.7%	13%
Slope	4.17	4.23	4.27
E_{max}	23 PeV	4 PeV	0.5 PeV

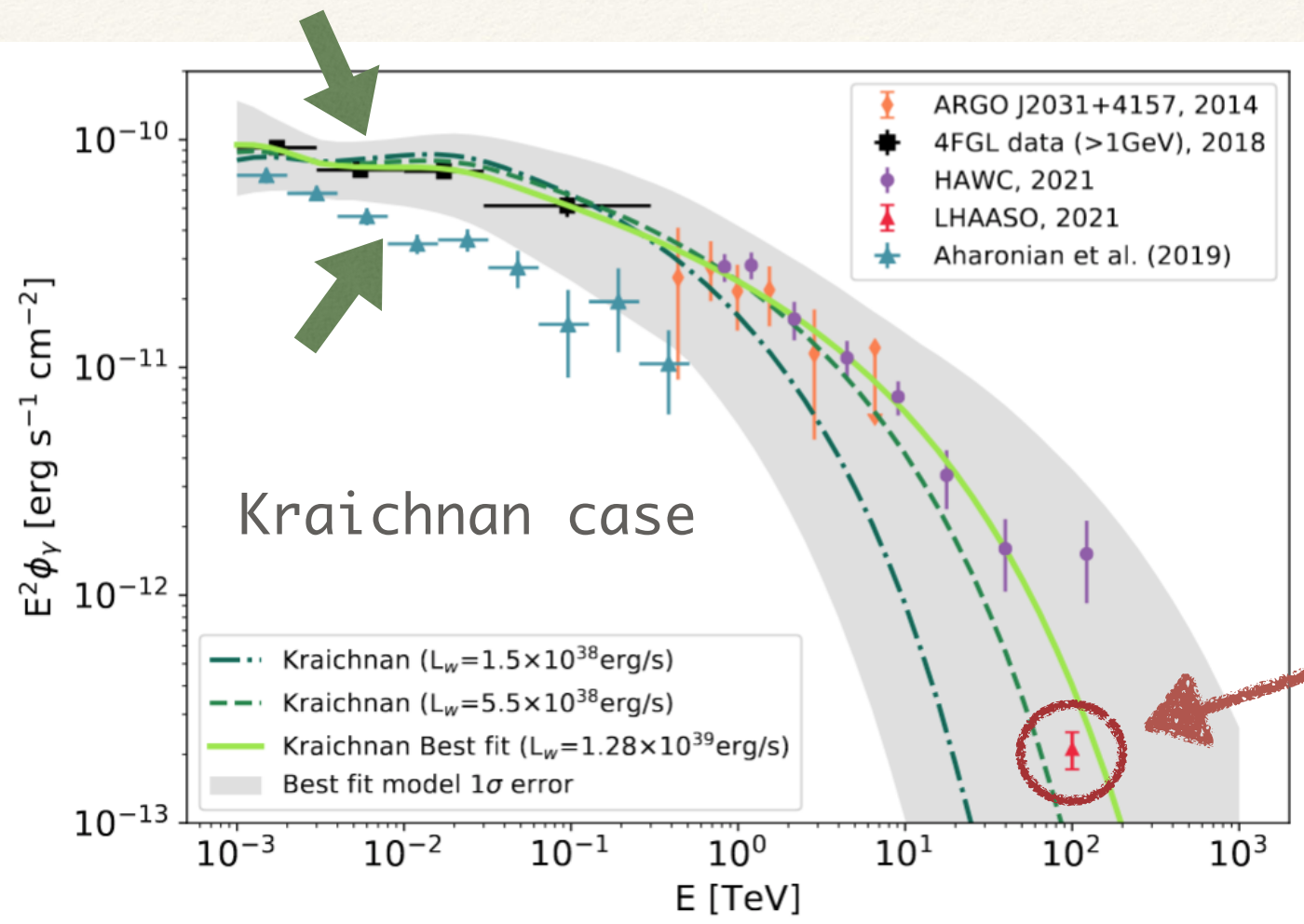
Unrealistically high

The most realistic scenario is something in between Bohm and Kraichnan



The case of Cygnus Cocoon

[S. Menchiari et al. in preparation]



Some caveats:

- ❖ Different analysis of Fermi-LAT data gives different results
- ❖ In comparing different experiments we need to correctly account for the different extraction area
- ❖ LHAASO data-point is not used for the fit because the extraction area is not specified

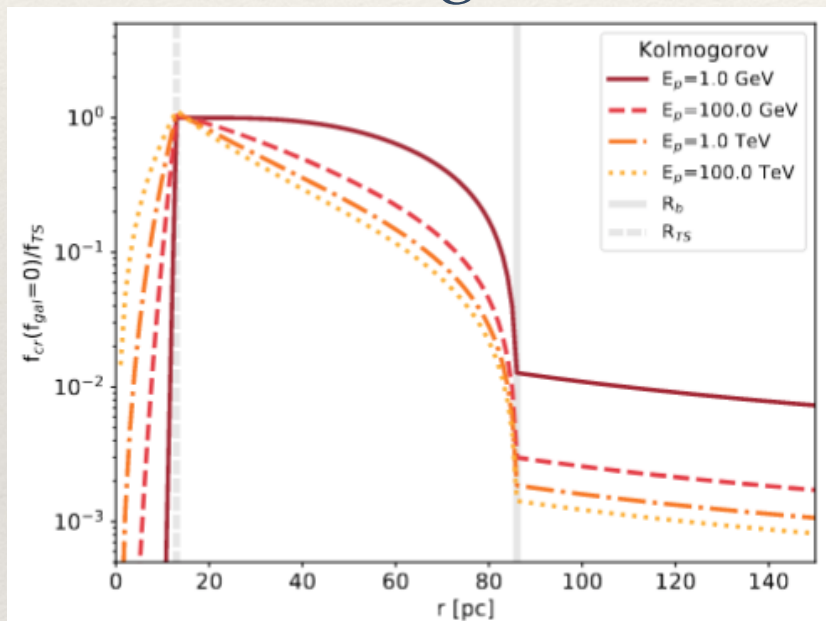
Better constraints requires a careful combined analysis of different experiments

CR radial profile

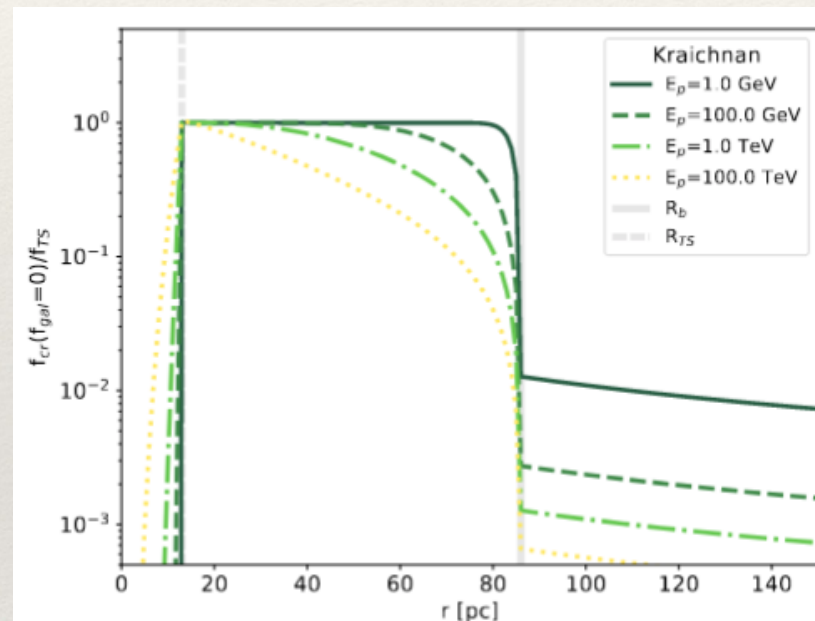
[S. Menchiari et al. in preparation]

The harder is the diffusion coefficient the flatter is the CR distribution

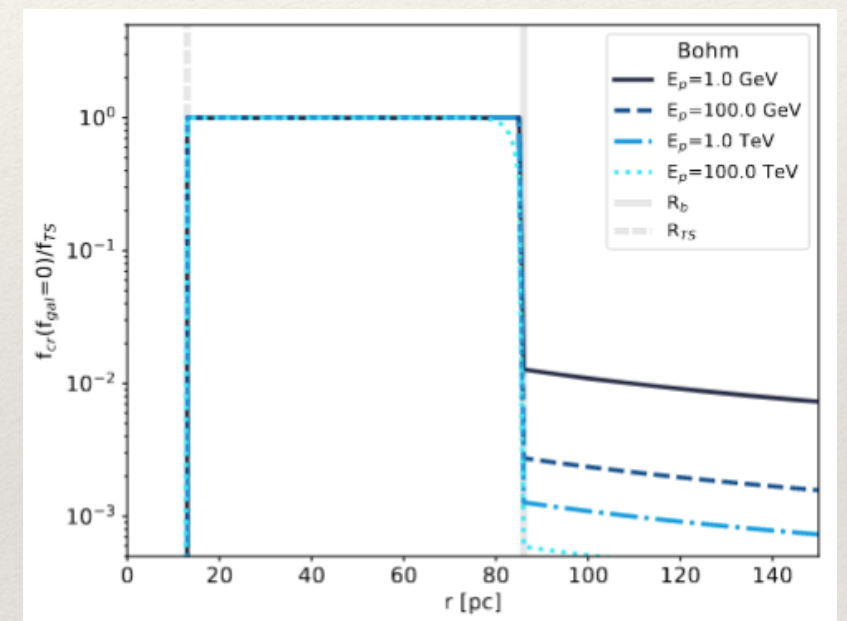
Kolmogorov



Kraichnan



Bohm

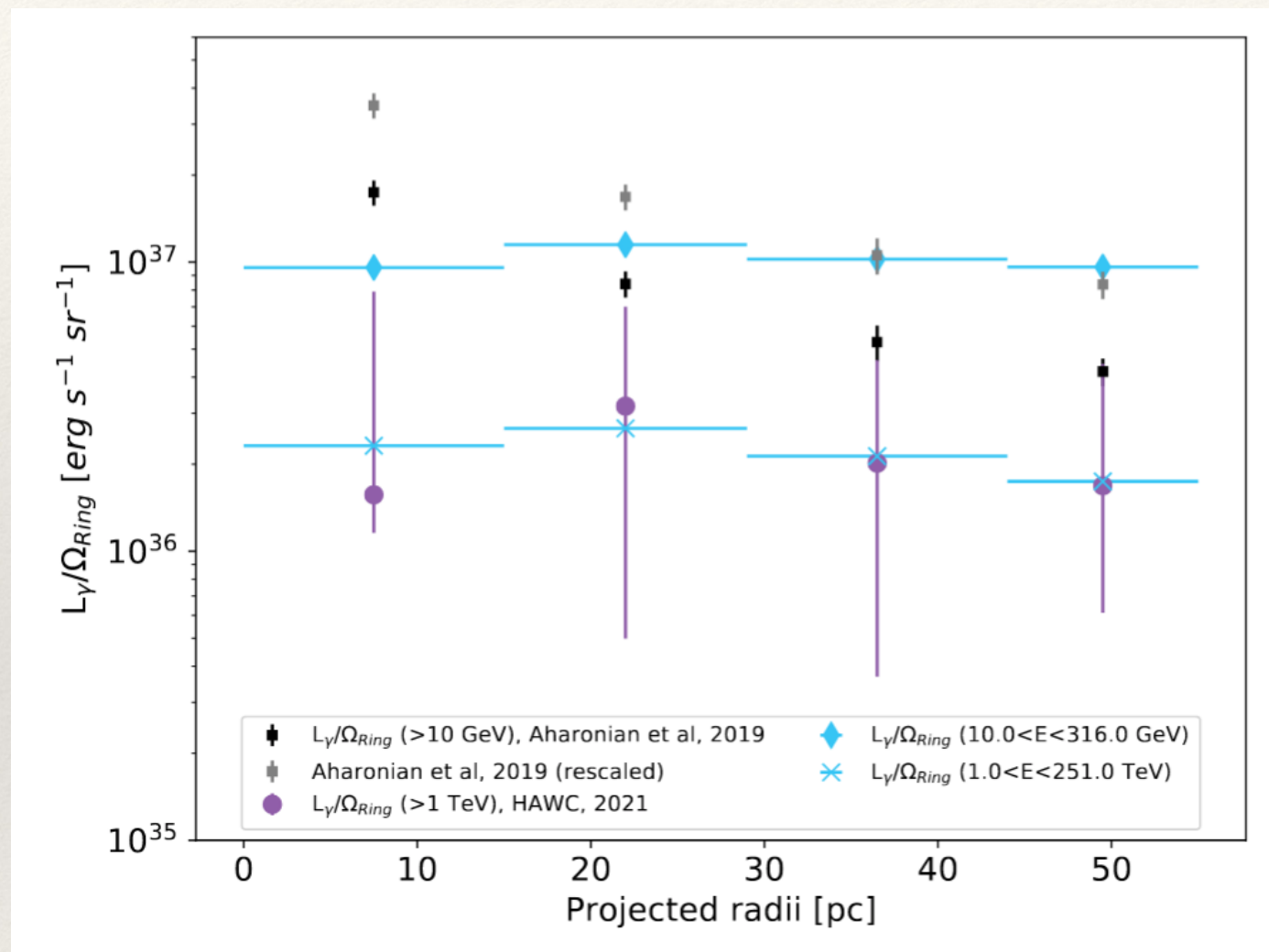


CR radial profile

[S. Menchiari et al. in preparation]

The line-of-sight integrated gamma-ray emission

Kraichnan
case



- ❖ Not compatible with $1/r^2$ inferred from FermiLAT data
- ❖ Compatible with HAWC data in TeV

Radial profile: advection vs. diffusion

What should be the CR spatial profile in stellar clusters?

1. Pure diffusion model from a stationary central source

$$f_{\text{CR}} = Q(E) \frac{4Dt}{\sqrt{\pi} r} e^{-\frac{r^2}{4Dt}} \propto \frac{1}{r} \quad \text{for } r < 4Dt$$

2. Transport in a wind-blown bubble from a stationary central source

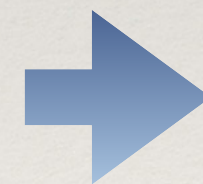
$$\text{Diffusion time: } t_{\text{diff}} \sim \frac{R^2}{4D(E)}$$

$$\text{Advection time: } t_{\text{adv}} \sim \frac{R}{v_w}$$

Upper limit on the diffusion coefficient can be estimated from gamma-ray luminosity

$$L_{\gamma}^{\text{pp}} \propto \xi_{\text{CR}} L_w n_{\text{bubble}} V_{\text{bubble}} \lesssim L_{\gamma}^{\text{obs}}$$

for Cygnus cocoon $\Rightarrow D \lesssim 100 D_{\text{gal}}$



$$t_{\text{diff}}(E) > t_{\text{adv}} \quad \text{for } E \lesssim 100 \text{ GeV}$$

In the Fermi-LAT energy range we do expect a flat CR profile

Conclusions

- ❖ Young stellar clusters are promising gamma ray sources
- ❖ YSC can significantly contribute to Galactic CRs
- ❖ Maximum energies can reach \sim PeV (but strong dependence on diffusion \Rightarrow Multi-wavelength fit required to better constrain B)
- ❖ Super-bubbles (= older SCs with stellar winds+ SNRs) may be the major contributors of Galactic CRs (but theoretical models still incomplete)
- ❖ Next generation IACT will probably detect many new stellar clusters (\sim several tens) (but extended sources with low surface brightness)

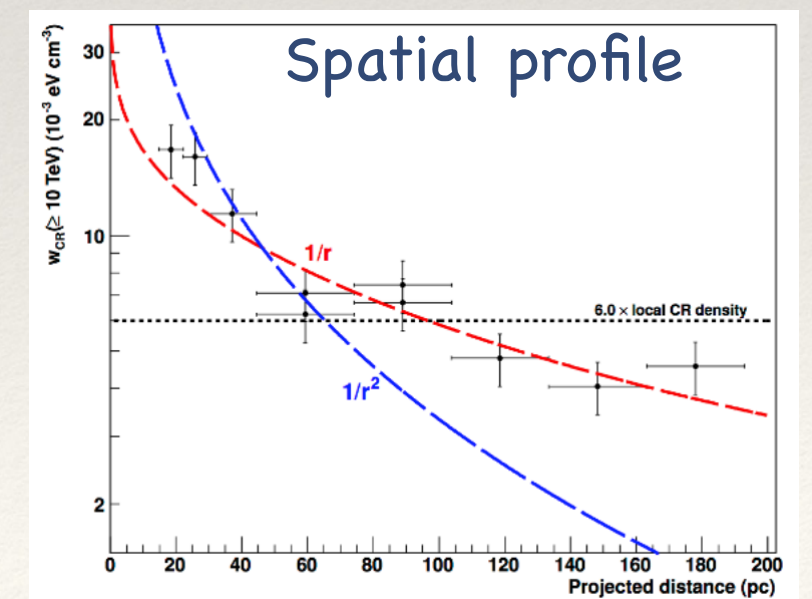
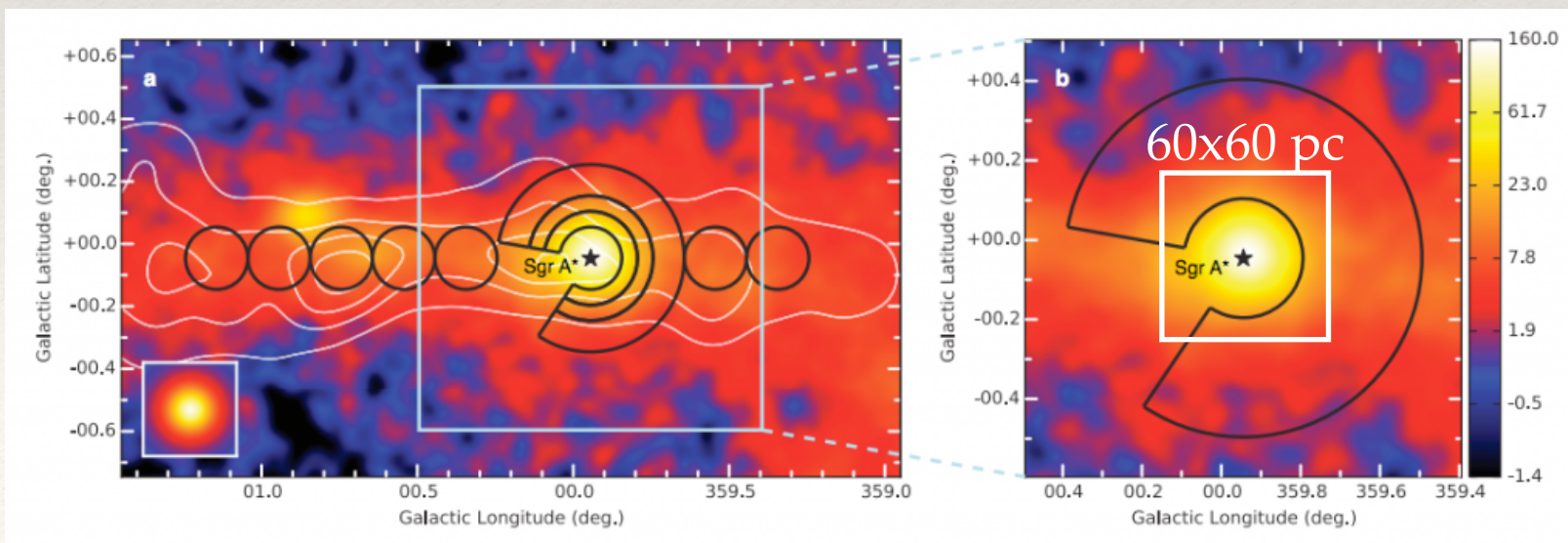
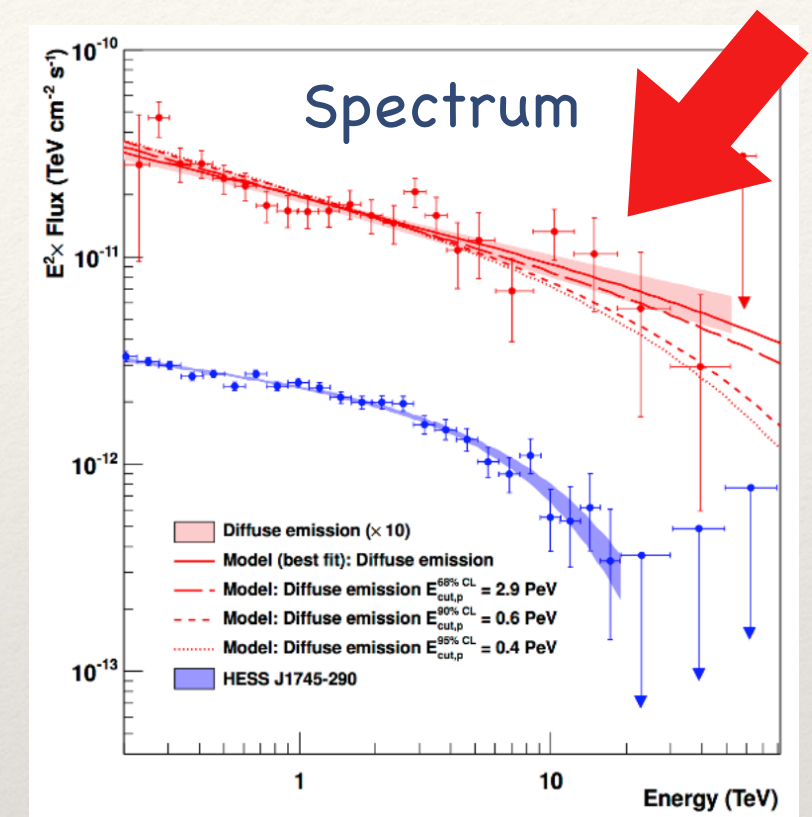
Backup slides

Possible role of YSC in the Galactic Center

[H.E.S.S. coll., Abramowski et al. Nat. 531 (2016)]

The Galactic Centre has been recognised as a PeVatron

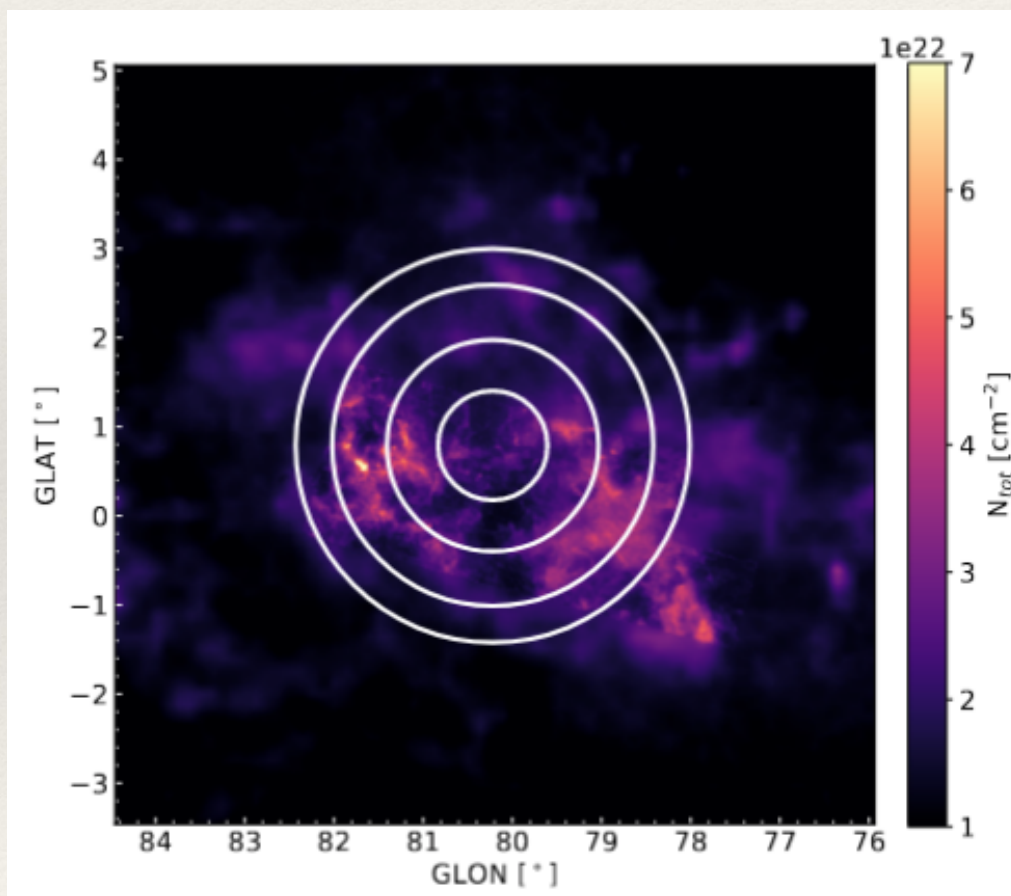
- ❖ Minimum proton energy > 0.4 PeV
- ❖ Spatial profile compatible with continuous emission
 - ➔ SNR disfavoured
- ❖ CR luminosity: $L_{\text{CR}}(> 10 \text{ TeV}) = 4 \times 10^{37} (D/10^{30} \text{ cm}^2 \text{ s}^{-1}) \text{ erg/s}$
(could be supplied by a powerful cluster wind if diffusion is suppressed)
- ❖ Stellar clusters in the GC region:
 - Arches (~ 30 pc from Sgr A*, Mass $\sim 10^4 M_{\odot}$, age ~ 2.5 Myr)
 - Quintuplet (~ 30 pc from Sgr A*, Mass $\sim 10^4 M_{\odot}$, age ~ 4 Myr)
 - Central cluster (~ 200 young stars at $r \lesssim 1$ pc from Sgr A* including ~ 30 WR stars) [e.g. von Fellenberg et al. (2022) and Poumard T. (2008)]



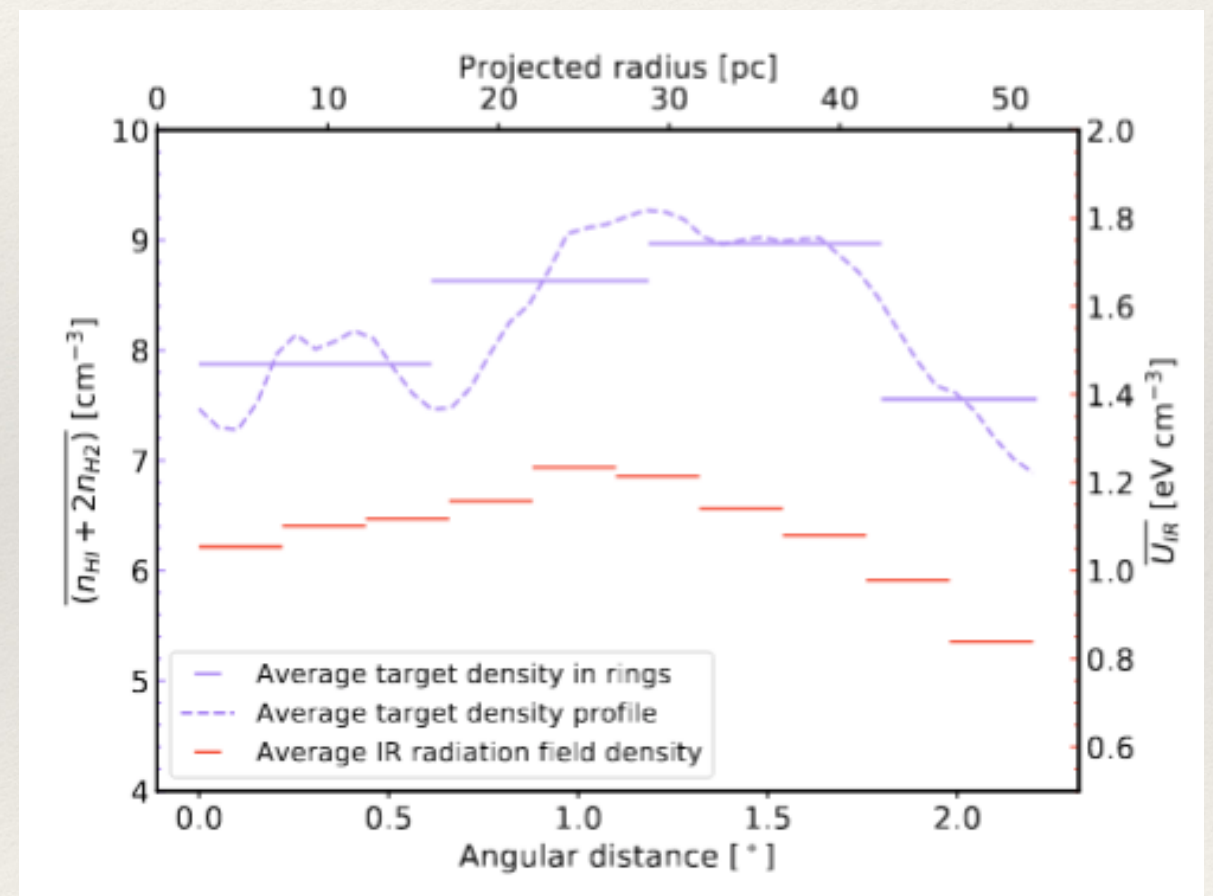
Gas and photons distribution

[S. Menchiari et al. in preparation]

Gas distribution from CO map

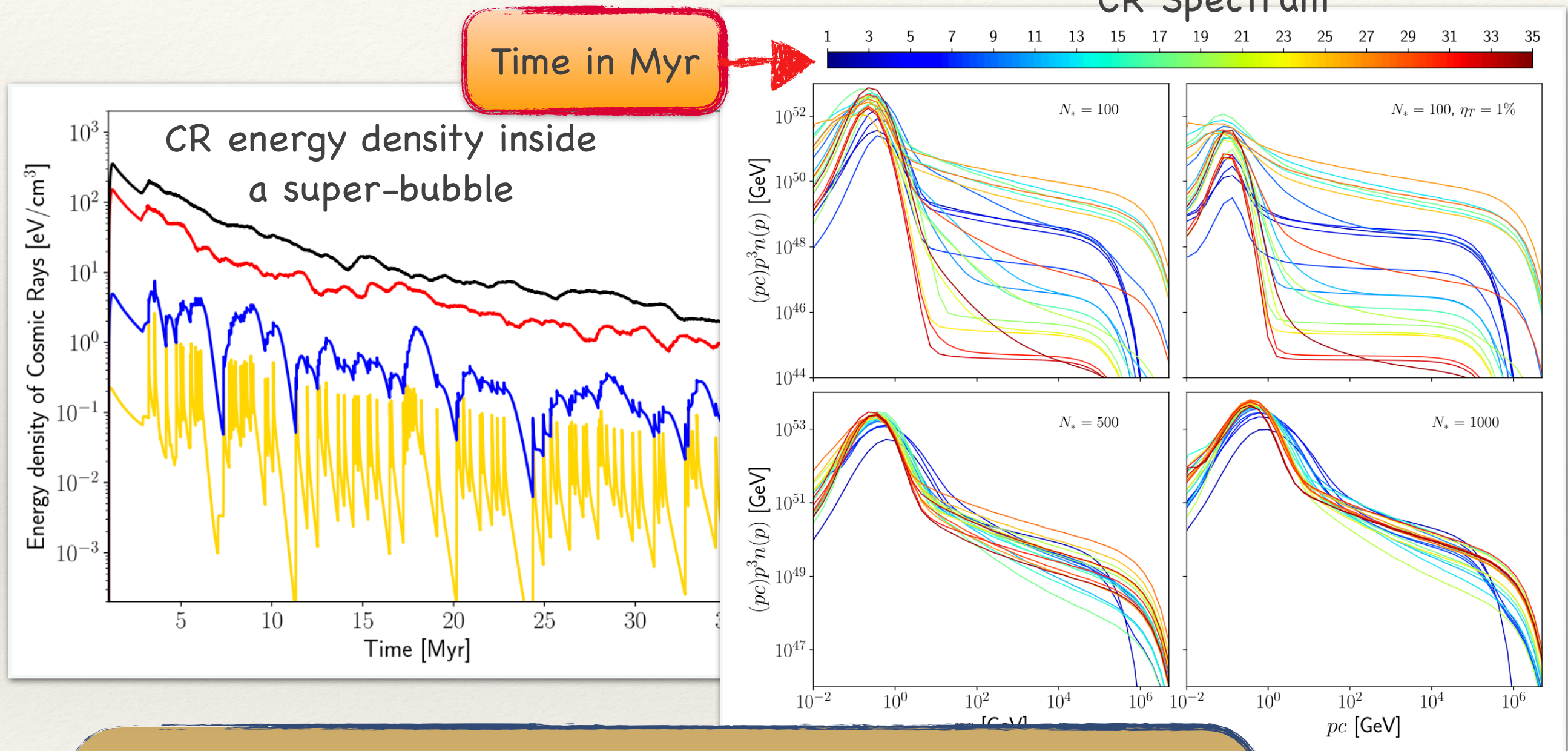


Photon background is dominated by IR radiation Star-light from Cyg. OB2 is negligible



Particle acceleration in super-bubbles: intermittency

Vieu et al. (2022): consider acceleration at WTS + SNR forward shock + turbulent acceleration



- ❖ Energetically Superbubble may produce the bulk of CRs
- ❖ The spectrum is not universal -> strong intermittency